



Contents lists available at ScienceDirect

Saudi Pharmaceutical Journal

journal homepage: www.sciencedirect.com

Original article

Plant-mediated green synthesis of gold nanoparticles using an aqueous extract of *Passiflora ligularis*, optimization, characterizations, and their neuroprotective effect on propionic acid-induced autism in Wistar rats

Najlaa S. Al-Radadi^{a,*}, Widad M. Al-Bishri^b, Neveen A. Salem^{b,c}, Shaimaa A. ElShebiny^c

^a Department of Chemistry, Faculty of Science, Taibah University, P.O. Box 30002, Al-Madinah Al-Munawarah 14177, Saudi Arabia

^b Department of Biochemistry, College of Science, University of Jeddah, Jeddah, Saudi Arabia

^c Department of Narcotics, Ergogenic Aids and Poisons, Medical Research and Clinical Studies Institute, National Research Centre, Cairo, Egypt

ARTICLE INFO

Keywords:

Sweet granadilla
Antioxidant
Anti-inflammatory
Gold nanoparticles
Autism

ABSTRACT

The current study was conducted to examine an innovative method for synthesizing gold nanoparticles (AuNPs) from an aqueous sweet granadilla (*Passiflora ligularis* Juss) *P. ligularis*. Furthermore, the synthesized AuNPs were used to explore their potential neuroprotective impact against propionic acid (PPA)-induced autism. A sweet granadilla extract was used to achieve the synthesis of AuNPs. The structural and dimensional dispersion of AuNPs were confirmed by different techniques, including UV-Vis spectrophotometer (UV-Vis), X-ray Diffraction (XRD) Pattern, Energy Dispersive X-ray (EDX), Zeta potential, and High-Resolution Transmission Electron Microscopy (HRTEM) analysis. The AuNPs mediated by *P. ligularis* adopt a spherical shape morphology and the particle size was distributed in the range of 8.43–13 nm without aggregation. Moreover, *in vivo*, the anti-autistic effects of AuNPs administration were higher than those of *P. ligularis* extract per second. In addition, the reduced anxiety and neurobehavioral deficits of AuNPs were observed in autistic rats which halted the brain oxidative stress, reduced inflammatory cytokines, ameliorated neurotransmitters, and neurochemical release, and suppressed apoptotic genes ($p < 0.05$). The alleviated antiapoptotic gene expression and histopathological analysis confirmed that the treatment of AuNPs showed significant neural pathways that aid in reducing tissue damage and necrosis. The results emphasize that the biomedical activity was increased by using the green source synthesis *P. ligularis* -AuNPs. Additionally, the formulation of AuNPs demonstrates strong neuroprotective effects against PPA-induced autism that were arbitrated by a range of different mechanisms, such as anti-inflammatory, antioxidant, neuromodulator, and antiapoptotic effects.

1. Introduction

Passion fruit is the general name given to several species of *Passiflora* (*Barbosa Santos et al., 2021*). The *Passiflora* genus has been considered to contain more than 500 species, most of which produce fruits for industrial processing and human consumption (*Bugallo et al., 2020*). A large number of these species may be found in tropical America, specifically in Ecuador, Brazil, Peru, Colombia, Paraguay, and Bolivia (*He et al., 2020*). Passion fruit is abundant in the vitamins B1, B2, and C, as well as fibers, minerals, beta-carotene, and pro-vitamin A (*de Oliveira et al., 2017*). Additionally, it also showed potent antifungal and antibacterial activities (*Ramli et al., 2020, Carmona-Hernandez et al.,*

2021).

P. ligularis are known for being low in fat and significantly rich in fiber, vitamins A, C, K, P, niacin (*Sampaio et al., 2022; Ryals et al., 2020*), carbohydrates, as well as phosphorus, iron, and calcium (*Ashok et al., 2020*). The plant sweet granadilla has several promising biological properties, including antimicrobial, antioxidant, hepatoprotective, anti-hypertensive, lung-protective, and anti-inflammatory activities, as well as anxiolytic-like anti-diabetic, sedative antidepressant activities (*Rai et al., 2022, Khalil and Tazeddinova, 2020, Sayago-Ayerdi et al., 2021*). They have been historically used to treat diseases like Alzheimer's, Cancer, Parkinson's, and liver disorder (*Ravi, 2021*). According to the photochemical investigations sweet granadillas contain flavonoids

Peer review under responsibility of King Saud University.

* Corresponding author.

E-mail address: nsa@taibahu.edu.sa (N.S. Al-Radadi).

<https://doi.org/10.1016/j.jsps.2023.101921>

Received 12 May 2023; Accepted 12 December 2023

Available online 15 December 2023

1319-0164/© 2023 Published by Elsevier B.V. on behalf of King Saud University. This is an open access article under the CC BY-NC-ND license (<http://creativecommons.org/licenses/by-nc-nd/4.0/>).

(isochaftoside, chrysin, homo orientin, orientin, swertisin), alkaloids (harmalol, harmol, harmine, harmaline), organic acids (butyric, formic, palmitic acid, and makicoleic), esters (ethylcaporate and butyrate), sugars (glucose and fructose), enzymes (phenolase and catalase) (da Fonseca et al., 2020; George et al., 2017). All of these substances have been allied to the scavenging of free radicals, reducing oxidative stress, and inhibiting the oxidation of biomolecules that cause deterioration of physiological activities (Boaventura et al., 2013). These substances can decrease post-prandial hyperglycemia and block the essential enzymes glucosidase and amylase, which offer possible treatments for diabetes mellitus (Saravanan and Parimelazhagan, 2014). When there is a lot of oxidative stress over a long period, cells may suffer severe injury. Degenerative and Chronic diseases like cancer, aging, arthritis, autoimmune disorders, and cardiovascular and neurological diseases are all greatly influenced by oxidative stress (Shinde et al., 2012). Many factors, including genetics, oxidative stress, the environment, immunology, and neurological factors, are known to contribute to autism spectrum disorder (ASD). ASD is a stereotypical central nervous system condition (CNS). Communication issues, repetitive behavior and narrow interests, hyperactivity (Sharma et al., 2019), digestive issues, irritability, aggression, sleep abnormalities, epilepsy, anxiety, and sensory processing disorders are common signs of ASD (Bhandari and Kuhad, 2015). Genetic and environmental variables are thought to have significant component in the etiology of ASD, even though it has not yet been properly developed (Hayretdag et al., 2020). A major part of neurodevelopmental disorders like autism is also controlled by the immune system. Other variables which might have a role in the progression of ASD were maternal obesity, cigarette smoking, air pollution, alcohol use, and maternal infections/immune activation (Bölte et al., 2019). Owing to the absence of facts about the pathophysiology, origin, and of symptoms associated with autism, it is not entirely curable. Modern synthetic drug therapy aims to relax patients and increase memory, but each drug used for this purpose has a unique profile of hazardous side effects. Hence, biological methods used for the formation of nanoparticles like plant extracts (flowers, leaves, bark, stems, seeds, fruit peels, etc.) have several advantages over toxic chemical processes, including environmentally friendly and biocompatibility with pharmaceuticals and other biomedical applications (Khandel et al., 2018, Al-Radadi, 2022a, Olawale et al., 2022). Nanoparticles are tiny particles with size ranges between 1 and 100 nm (Satzer et al., 2016, Ijaz et al., 2020). They are frequently synthesized using either top-down or bottom-up methods (Al-Radadi and Al-Youbi, 2018a, Fu et al., 2018, Yucel et al., 2020). Due to their diverse chemical properties, nanoparticles are valuable in a wide range of industries, including optics and medicine, where they can be utilized to treat diseases (Deshmukh et al., 2019). Plants are used in the biogenic synthesis method to yield nanoparticles (Rozhin et al., 2021). The green synthesis may offer nanoparticles with more precisely defined sizes and morphologies as compared to certain other physicochemical ways of synthesis (Gebreslassie and Gebretnsae, 2021, Al-Radadi et al., 2022). The fundamental virtue of adopting plant-based synthesis techniques over conventional physical and chemical techniques is that they are more cost-effective, easier to scale up, and more environmentally friendly for synthesizing large amounts of nanoparticles. Additionally, these techniques do not involve the use of hazardous chemicals, high pressures, or extreme temperatures (Al-Radadi and Adam, 2020, Kujur and Daharwal, 2021, Rónavári et al., 2021, Al-Radadi, 2022b). Metal nanoparticles (MNPs) may be employed to direct a natural supplement into a particular organ that is affected, improving drug delivery, selectivity, efficacy, and safety and lowering medication dosage (Al-Radadi, 2018, Al-Radadi, 2021a,b). Due to their small particle size and high loading capacities, they aid in enhancing the herbal medication's solubility and concentrating the drug in a specific affected area, which results in better efficacy (Bhaskar et al., 2010, Sachan and Gupta, 2015, Al-Radadi and Al-Youbi, 2018b). Therefore, the synthesis of metal nanoparticles has attracted significant interest in a wide range of biomedical fields, including cancer therapies,

antibacterial agents, and gene transplantation (Patra and Baek, 2015, Yaqoob et al., 2020, Al Jahdaly et al., 2021). The nanoparticles synthesis for medical purposes has to be biocompatible and either low-toxic or non-toxic (Ratan et al., 2020). Metal nanoparticles like platinum, Palladium, gold, and silver nanoparticles have undergone extensive testing on humans (da Silva et al., 2011, Schröfel et al., 2014, Al-Radadi, 2022c, Al-Radadi, 2019, Faisal et al., 2021, Prakash Patil et al., 2021, Abdullah et al., 2022, Al-Radadi, 2022d). Owing to its biocompatibility and surface modifiability, the gold metal, which is considered to be the most recognized metal nanoparticle for health applications, will be our choice (Moore and Chow, 2021). Gold nanoparticles (AuNPs) have received a lot of attention because they may interact with light via surface plasma resonance (SPR) (Shedbalkar et al., 2014, Sibuyi et al., 2021). Moreover, AuNPs have antibacterial, antioxidant, and catalytic properties. Several cancer cell lines have been successfully treated using natural sources for the formation of AuNPs (Kajani et al., 2016, Khandanlou et al., 2018, Khan et al., 2019, Rajeshkumar et al., 2021). Due to their multifunctional properties in detection, therapeutics, surface chemistry, and imaging, AuNPs have employed in different fields such as material sciences, chemistry, medicine, physical, and life sciences (Panzarini et al., 2018, Barabadi et al., 2020, Al-Radadi, 2022e, Al-Radadi, 2023). Moreover, there is no specific literature available on aqueous *Passiflora ligularis* extracts used for the synthesis of AuNPs. Therefore, the aim of the current investigation was used to explore the effectiveness of an aqueous extract *P. ligularis*, as a biological source to treat a wide range of diseases and may serve as an ideal goal for the identification of active natural compounds utilizing activity isolation. The optical, morphological, elemental, and structural properties of synthesized *P. ligularis*-AuNPs were characterized by different techniques including, UV-Vis, XRD, HRTEM, Zeta potential, and EDX. Furthermore, the *P. ligularis*-AuNPs were used to examine the potential neuroprotective impact against propionic acid-induced autism in rats by exploring the oxidative stress, behavioral, inflammatory, and gene expression markers (Scheme.1).

2. Materials and methods

2.1. Preparation of sweet granadilla Extract and green synthesis of *p. ligularis*-AuNPs

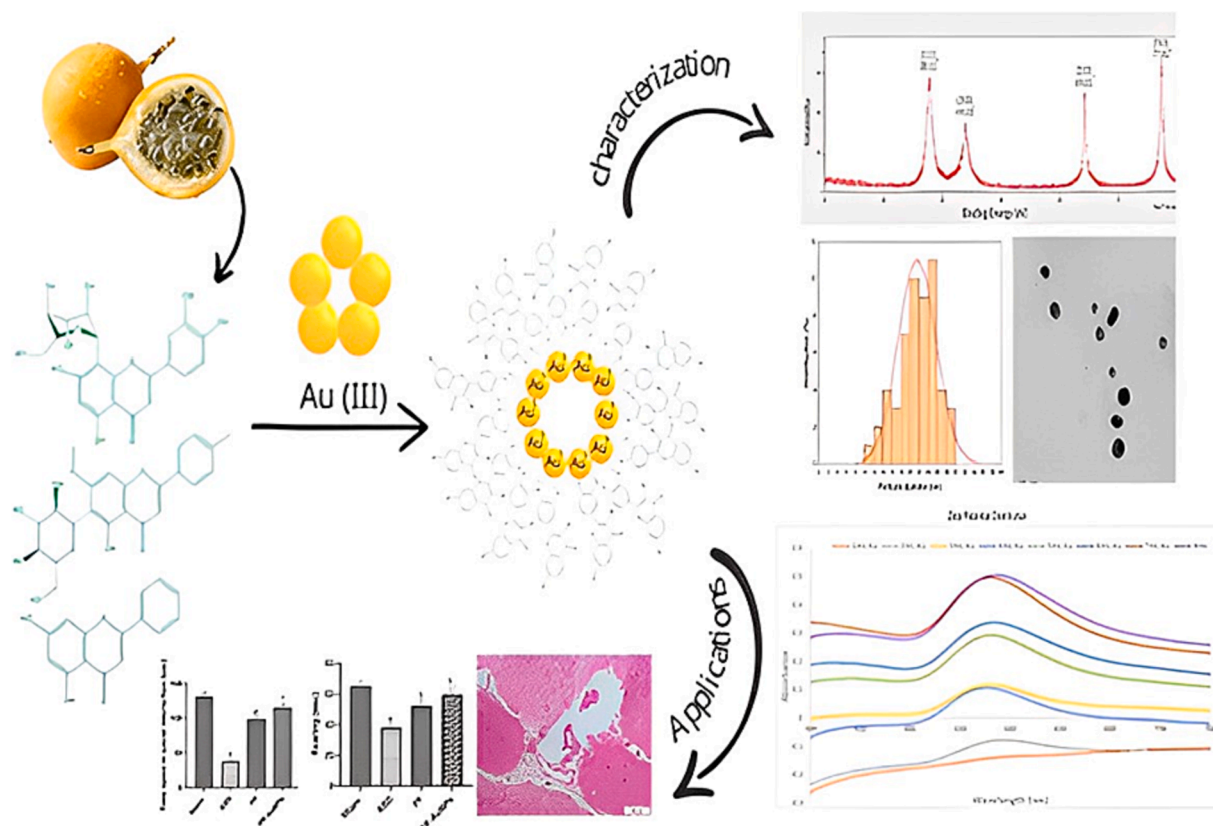
The fresh sweet granadilla was purchased from a local market. The sweet granadilla was rinsed by distilled water to get rid the dust and other contaminated particles that were used to prepare an aqueous extract. The (5 gm) sweet granadilla pulp was mixed with (70 mL) of distilled water in a cleaned dry glassware and was boiled in a flask for a few min. The extract was cooled down and then filtered through Whatman filter paper. An aqueous extract was served as reducing and stabilizing agent for the synthesis of *P. ligularis*-AuNPs. After that, different volume of an aqueous extract was mixed into different ratios of (1×10^{-3} M) solution of precursor tetra chloroauric acid ($\text{HAuCl}_4 \cdot 3\text{H}_2\text{O}$) (Sigma Aldrich) to achieve the optimum synthesis of *P. ligularis*-AuNPs. The reaction mixture was stirred until the color of the solution changed, and UV-Vis spectrophotometry was employed to confirm the formation of *P. ligularis*-AuNPs.

2.2. Optimization studies for *p. ligularis*-AuNPs synthesis

To determine the stability of synthesized *P. ligularis*-AuNPs from sweet granadilla extract, several optimum factors were investigated, including the volume of sweet granadilla extract, volume of ($\text{HAuCl}_4 \cdot 3\text{H}_2\text{O}$) solution, temperature, pH, and reaction time. The final solution was characterized by UV-visible absorption spectra and verified by HRTEM images.

2.2.1. Optimization of extract volume

To optimize the synthesis of *P. ligularis*-AuNPs, different volumes (1



Scheme 1. Green Synthesis of AuNPs and *P. ligularis*.

mL, 2 mL, 3 mL) of sweet granadilla extract were mixed to (7 mL) of ($1 \times 10^{-3} M$) ($H AuCl_4 \cdot 3H_2O$) in a reaction that was kept at room temperature ($25^\circ C$) for around 6 h.

2.2.2. Optimization of $H AuCl_4 \cdot 3H_2O$ Volume

The volume effects of ($H AuCl_4 \cdot 3H_2O$) were investigated by reacting (3 mL) of sweet granadilla extract with (1 mL, 2 mL, 3 mL, 4 mL ...7 mL) volumes of ($H AuCl_4 \cdot 3H_2O$) solution simultaneously for about 6 h at room temperature ($25^\circ C$).

2.2.3. Optimization of reaction time

To determine the impact of time interval, the absorption spectra of *P. ligularis*-AuNPs formed during the reaction medium with the optimum volume of ($H AuCl_4 \cdot 3H_2O$) and sweet granadilla extract solution were examined over a range of reaction times (1–6 h) at ($25^\circ C$) room temperature.

2.2.4. Optimization of pH

With the optimal amount of sweet granadilla extract and ($H AuCl_4 \cdot 3H_2O$) solution, the reaction mixture was optimized by pH that was evaluated at various levels of pH (1, 2, 3, 4, and 6) subsequently 6 h of the reaction, at ($25^\circ C$) room temperature.

2.2.5. Optimization of temperature

P. ligularis-AuNPs were stabilized by maintaining the reaction under the aforementioned optimal conditions at varying temperatures ($15^\circ C$, $20^\circ C$, $25^\circ C$, $30^\circ C$, $35^\circ C$) for approximately 6 h.

2.3. Characterization of AuNPs

The UV–visible spectroscopy (Shimadzu, UV-2600) was employed to confirm the synthesis of AuNP son wavelength ranges between 400 and 800 nm, at regular intervals. After that, the sample of AuNPs was dried

for two days at ($25^\circ C$) in an oven to eliminate the moisture. The dry sample was subsequently acquired and analyzed using powder XRD to ascertain the crystalline morphology of AuNPs. The data was collected using PANalytic EMPYREAN at (45 kV), (40 mA), over a range of (2θ) = (20 – 80°) with a scanning speed of (2θ /min). HRTEM (high-resolution transmission electron microscopy) and the zeta potential for stability of *P. ligularis*-AuNPs were used to examine the size, dispersion, and morphology of the AuNPs. The surface stability, elemental composition, and size of the synthesized AuNPs were investigated using the EDX analysis.

2.4. Animals

The NRC (National Research Centre), in Cairo, Egypt provided 70 male Wistar rats, each weighing 200 ± 20 g. The food and water used in laboratories were provided to the rats, which were housed under standard conditions. All experimental procedures followed the guidelines set by the National Research Council Ethics Committee and the National Institutes of Health for the ethical treatment and possession of experimental animals (Publication No. 85–23, revised 1985).

2.5. Acute Toxicity study

The optimum *P. ligularis*-AuNPs formulation was compared to a solution of *P. ligularis* extract in an *in vivo* acute toxicity assay to determine their safety on rats after their administrations. 30 Wistar rats weighing 180 ± 20 gm were used. Rats were divided into 6 groups 5 rats each. The aqueous extract *P. ligularis* was administered to three groups at concentrations of (10, 20, and 40 mg/kg) wt orally by gastric lavage, while the other three groups received *P. ligularis*-AuNPs at concentrations of (2, 4, and 8 ppm). The lethal dose (LD50) over a 24-hour interval that killed half the animals was recorded for both formulations. The rats were allowed free access to rat food and water and underwent a week of

acclimation prior to the experiment. The Animal Care and Use Committee of NRC, Cairo, Egypt, confirmed their approval of the study's ethical practices and principles (Panzarini et al., 2018, Barabadi et al., 2020).

2.6. Experimental model of intracerebroventricular PPA-Induced Autism

Ketamine/xylazine cocktail (0.1 ml/100 gm rat) was used to anesthetize the rats. To expose the skulls, the animals' heads were shaved, cleansed, and cut. A midline sagittal incision was made in each rat's scalp while placed in a frame of stereotaxic. To access the anterior section of the caudoputamen, the skull was punctured by a burr hole (Stereotaxic coordinates: anterior/posterior 1.4 mm; medial/lateral 1.8 mm; dorsal/ventral 3.0 mm). A plastic ear pin was used to lock a cannula that measured (2.5 cm) in length. A fixative was then placed on top of the burr hole following its being sealed off with dental cement. An antibiotic (betadine) was frequently applied after the layer was sutured. Then (1M) propionic acid (PPA) solution was diluted by phosphate buffer saline (PBS) to a (4 μ l) injection volume and infused over the period days 1st to 7th day for 10 min. The intracerebrally (ICV) injection was introduced to sham animals that were the same as PBS (MacFabe et al., 2007).

2.7. Experimental design

Rats were dispensed into 4 groups; each group comprised 10 animals. Group (1) Sham control: PBS (ICV). Group (2) ASD group: PPA (ICV). Group (3) *P. ligularis* group (PPA + *P. ligularis* extract $\frac{40\text{mg}}{\text{kg}}$ b. wt p.o). Group (4) *P. ligularis*-AuNPs group (PPA + *P. ligularis*-AuNPs 2ppm/ml p.o). The total duration of the study was 28 days. From day 1st to day 7th PPA was administered ICV. *P. ligularis* and *P. ligularis*-AuNPs were chronically administered from day 8th to the end of the study (day 28). Neurobehavioral parameters were measured 28 days after ICV injection of PPA (reciprocal social interaction, stereotypic behavior, open field, and elevated plus maze). The brains of all the rats were removed and divided into two halves under deep ether anesthesia conditions. The first part was processed for further histological analysis by being paraffin-embedded and formalin-fixed. To achieve a final concentration of 10 %w/v, the remaining half was homogenized with (0.1M) phosphate buffer saline at pH 7.4 and centrifuged at (3000xg) for 15 min at (4 °C). Further, the biochemical analyses were performed using the resulting supernatant.

2.8. Neuro-behavioral assessment

The reciprocal social interaction, open field, elevated plus maze, and stereotypic behavior tests were carried out on day 28 after the PPA injection to evaluate social deficiencies specific to autism.

2.8.1. Reciprocal social interaction

Observe the behavior of two unfamiliar rats engaged in social interaction in a standard arena for 5 min. Various parameters were observed for social contact. The social parameters include (walking closely behind the other, push-crawl, and keeping pace) (Silverman et al., 2010).

2.8.2. Stereotypic behavior

The ASD-induced rats in a social environment and spraying their backs and necks with a fine water mist allows investigators to notice a nonsocial parameter known as recurrent self-grooming in the animals. Several spontaneous stereotypes behavioral can be observed in rats, such as jumping, self-grooming, and circling. All through the 5 min session was used to determine the total amount of time interval for grooming the body and the head (Moretti et al., 2005).

2.8.3. Elevated Plus-Maze

To explore the behavior of autistic rats related to anxiety, the analysis of elevated plus-maze was carried out. In this, the rats were kept in a typical elevated plus maze for 15 min, which was composed of a device (plus shaped) with two opposite enclosed arms and two open arms and (60 × 5 × 30 cm set at a right angle. The amount of time that was spent in each arm was determined (Hogg, 1996).

2.8.4. Open-Field test

To measure anxiety and nonselective attention, the open field test was carried out as previously reported by (Han et al., 2012). The open field apparatus typically measures (50 × 50 × 40 cm) and was filled with one rat per slot. The subject had five minutes to examine the arena. The number of entries in the center area, grooming, rearing times and distance traveled were all measured.

2.9. Biochemical investigation

2.9.1. Brain oxidative stress markers

TBARS (Thiobarbituric acid reactive compounds) in samples of brain tissue were measured to determine the amount of lipid peroxidation (Placer et al., 1966). The method of Ellman was used to assess brain glutathione (GSH) (George and Biophysics, 1959). In addition, the Marklund-described method was used to measure brain superoxide dismutase (SOD) activity (Marklund et al., 1985).

2.9.2. Brain inflammatory cytokines

The assay Enzyme-linked immunosorbent were employed to record the tumor necrosis alpha (TNF- α) and brain interleukin beta (IL-1 β) using a and an ELISA kit (Invitrogen Corporation in Camarillo, California) and microtiter plate reader (Fisher Biotech, Germany) in accordance with the procedures of Kitaura (Kitaura et al., 2004), and Tamaoki (Tamaoki et al., 1999), respectively.

2.9.3. Brain neurotransmitters

The high-performance liquid chromatography (HPLC) system was an Agilent Technologies 1100 series with a quaternary pump (Quat pump, G131A model) was used to measure the levels of brain dopamine, glutamate (glu), and serotonin (5-hydroxytryptamine, 5-HT). The ODS-reversed phase column (C18, 25x0.46 cm i.d. 5 μ m) was used to accomplish separation. A flow rate of 1 $\frac{\text{ml}}{\text{min}}$ was used to deliver the mobile phase, which was composed of a 97/3 ($\frac{\text{v}}{\text{v}}$) mixture of methanol and potassium phosphate buffer. The injection volume was (20 mL) and UV detection was carried out at 270 nm. The neurotransmitter concentration was calculated by using a peak area-based external standard approach. The concentration of the sample was directly determined from a linear standard curve (Salem et al., 2018).

2.9.4. Neurochemical parameters

Brain Myelin basic protein (MBP) and Extracellular signal-regulated protein kinase (ERK) were measured using a microtiter plate reader (Fisher Biotech, Germany) and ELISA kit (Invitrogen Corporation Camarillo, CA, USA) as followed by (Bernard et al., 2002, Choi et al., 2016) respectively.

2.10. Expression analysis of Apoptosis-Related genes

2.10.1. Extraction of Total RNA and cDNA synthesis

The Trizol® Reagent kit (Invitrogen, Germany) was employed to collect the total RNA (ribonucleic acid) from the brain tissues of rats. The instructions of the manufacturer were followed for the isolation technique. The complementary DNA (cDNA) originated by replicating the RNA that was obtained from brain tissue. The Revert Aid TM First Strand cDNA Synthesis Kit (MBI Fermentas, Germany) protocols were followed to produce a reaction volume of (20 μ l). Then, DNA product

was stored at (-20 °C) until DNA amplification.

2.10.2. Quantitative Real-Time-PCR (qRT-PCR)

The degree of cDNA replication and expression of the investigated genes in the rat population was assessed using a quantitative real-time PCR device (Applied Biosystem, USA). The $2^{-\Delta\Delta CT}$ approach were used to assess the comparative quantification of the targeted (Bcl2, Caspase-3, Bax) that were a reference to the (β -Actin).

2.11. Histopathological investigation

In the histopathological examination, the brain samples were fixed in 10% formol-saline, immersed in paraffin, subdivided into (5 μ m thick) sections with a microtome (Leica, Berlin, Germany), put on a microscope slide, stained with eosin and hematoxylin Stain and then examined under a light microscope.

2.12. Statistical analysis

The data were displayed as mean \pm SE of the mean. The data were subjected to a one-way analysis of variance (ANOVA) using the Statistical Package for the Social Sciences (SPSS) version 11 software, and Duncan post hoc tests with significance levels of ($p < 0.05$) were used to compare the results.

3. Results

3.1. *P. ligularis*-AuNPs production under different conditions and its characterization using UV-Visible and HRTEM analysis

The formation of gold nanoparticles was accomplished under a wide range of conditions, including different pH levels, different volumes of sweet granadilla extract, and various concentrations of ($\text{HAuCl}_4 \cdot 3\text{H}_2\text{O}$) solution. The formation of AuNPs with the sweet granadilla extract was indicated by changing the color of the reaction mixture to ruby red. However, a distinctive peak between AuNPs525 and 570 nm was visible in *P. ligularis*-AuNPs, which confirmed the synthesis of gold

nanoparticles (Aljabali et al., 2018, Ismail et al., 2018, Al-Radadi, 2022e). The synthesized *P. ligularis*-AuNPs provide additional evidence by examining HRTEM images (Fig. 6).

3.1.1. Effect of extract volume

The effect of extract volume on optimum synthesis of *P. ligularis*-AuNPs was carried out in a series of reactions by using different volumes of sweet granadilla extract (1 mL) to (3 mL) with a constant volume (7 mL) of (1×10^{-3} M) ($\text{HAuCl}_4 \cdot 3\text{H}_2\text{O}$). The reduction of Au ions was formed by allowing the reaction mixture for approximately 6 h at room temperature. Further, the UV-Vis absorption spectra were monitored to record the surface plasmon resonance peak intensity that was amplified and turned to be sharper by expanding the amount of extract sweet granadilla between (1 mL) to (3 mL) after 6 h of reactions (Fig. 1) (Gurunathan et al., 2014, Paul et al., 2014, Das et al., 2015, Majumdar et al., 2016). The results revealed that the optimum volume (2 mL) of sweet granadilla extract was suitable for the synthesis of *P. ligularis*-AuNPs which was confirmed by a UV-visible absorption analysis. Fig. 1 showed the highest SPR peak for 2 mL extract, whereas the spherical shape of the AuNPs was further demonstrated through HRTEM images of the stable *P. ligularis*-AuNPs as shown in Fig. 6.

3.1.2. Effect of $\text{HAuCl}_4 \cdot 3\text{H}_2\text{O}$ volume

The optimum *P. ligularis*-AuNPs synthesis was achieved using the volume effect of ($\text{HAuCl}_4 \cdot 3\text{H}_2\text{O}$) which was examined by changing the volumes of (1×10^{-3} M) ($\text{HAuCl}_4 \cdot 3\text{H}_2\text{O}$) (1–8 mL) at constant volume of sweet granadilla extract (2 mL) at room temperature for 6 h. The impact of ($\text{HAuCl}_4 \cdot 3\text{H}_2\text{O}$) on synthesized *P. ligularis*-AuNPs was evaluated using UV-Vis analysis. The absorption spectra of UV-Vis indicated a weak absorption peak intensity at 556 nm for (5 mL) ($\text{HAuCl}_4 \cdot 3\text{H}_2\text{O}$) solution. Additionally, UV-Vis absorption indicated a high peak intensity at a wavelength to 559 nm when the volume was increased to (7 mL), but in (8 mL) the peak intensity shifted towards the red area (bathochromic) at a wavelength to 566 nm. Therefore, the optimal volume was (7 mL), as shown in (Fig. 2) (Milaneze et al., 2014).

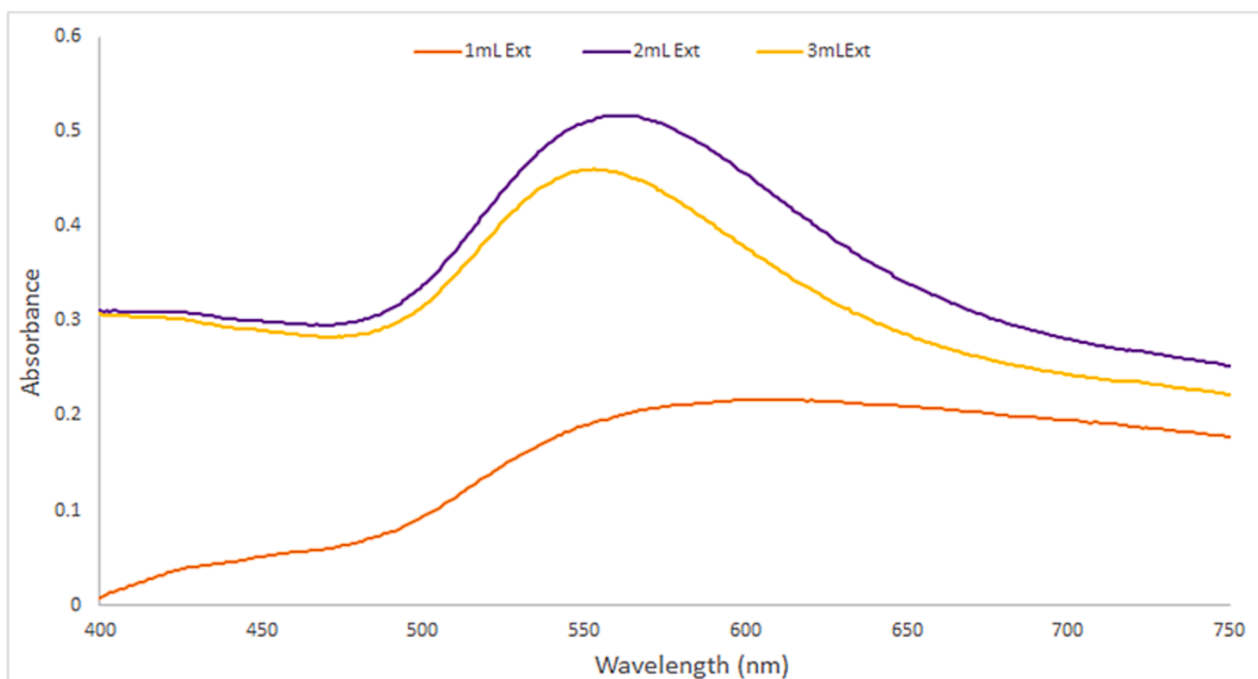


Fig. 1. UV-Vis absorption of gold nanoparticles by varying the volume of *P. ligularis* extract (1–3 mL) with (7 mL) ($\text{HAuCl}_4 \cdot 3\text{H}_2\text{O}$) (1×10^{-3} M) after 6 h and at room temperature 25 °C..)

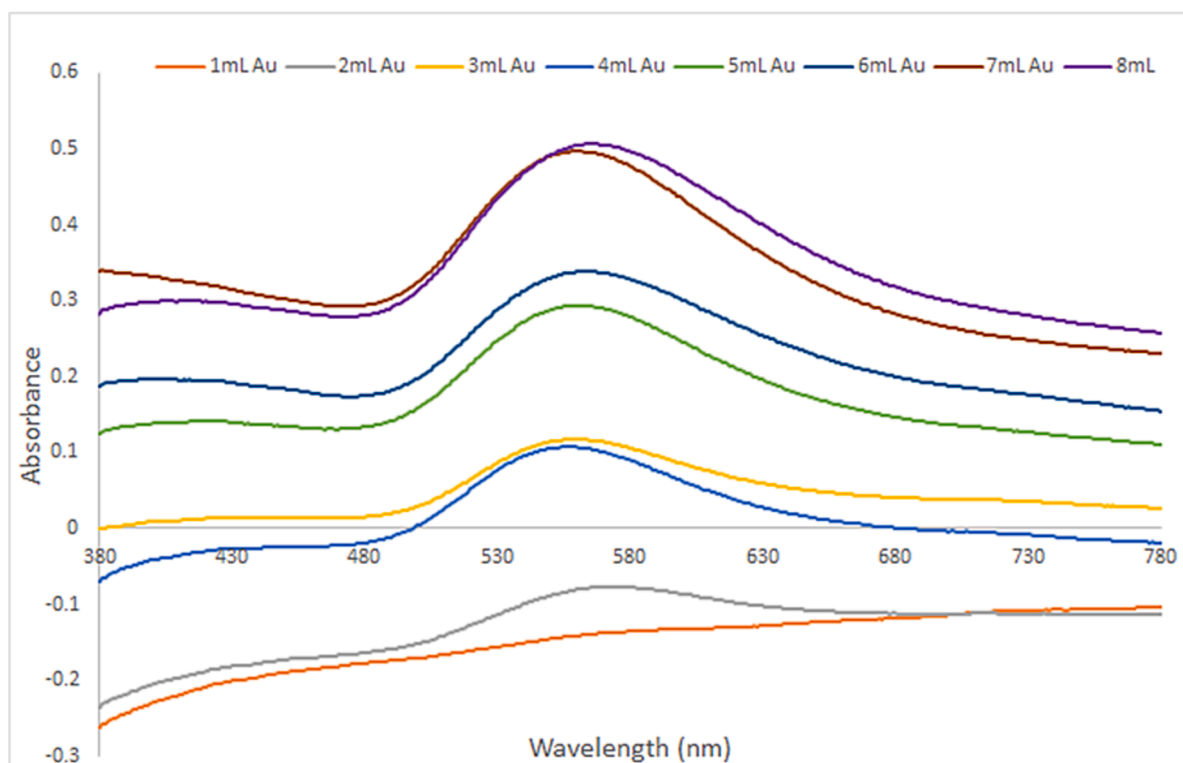


Fig. 2. UV-Vis absorption of gold nanoparticles by varying the volumes of (HAuCl₄·3H₂O) (1×10^{-3} M) (1–8 mL) with (2 mL) of *P. ligularis* extract after 6 h and at room temperature (25 °C..)

3.1.3. Effect of reaction time

The reaction of manufactured *P. ligularis*-AuNPs was observed by UV-vis spectroscopy during a batch reaction with (2 mL) *sweet granadilla* extract and (7 mL) (1×10^{-3} M) (HAuCl₄·3H₂O) at room temperature and for a period of 6 h. It was observed that the absorption peaks

intensity of the synthesized nanoparticles was likewise enhanced by increasing reaction time and becoming stronger and sharper at 6 h (Fig. 3) (Murad et al., 2018, Aji et al., 2019, Dudhane et al., 2019, Al-Radadi, 2023). Furthermore, the absorbance vs. reaction time graph represents that the peaks absorption become increases faster up to 4 h,

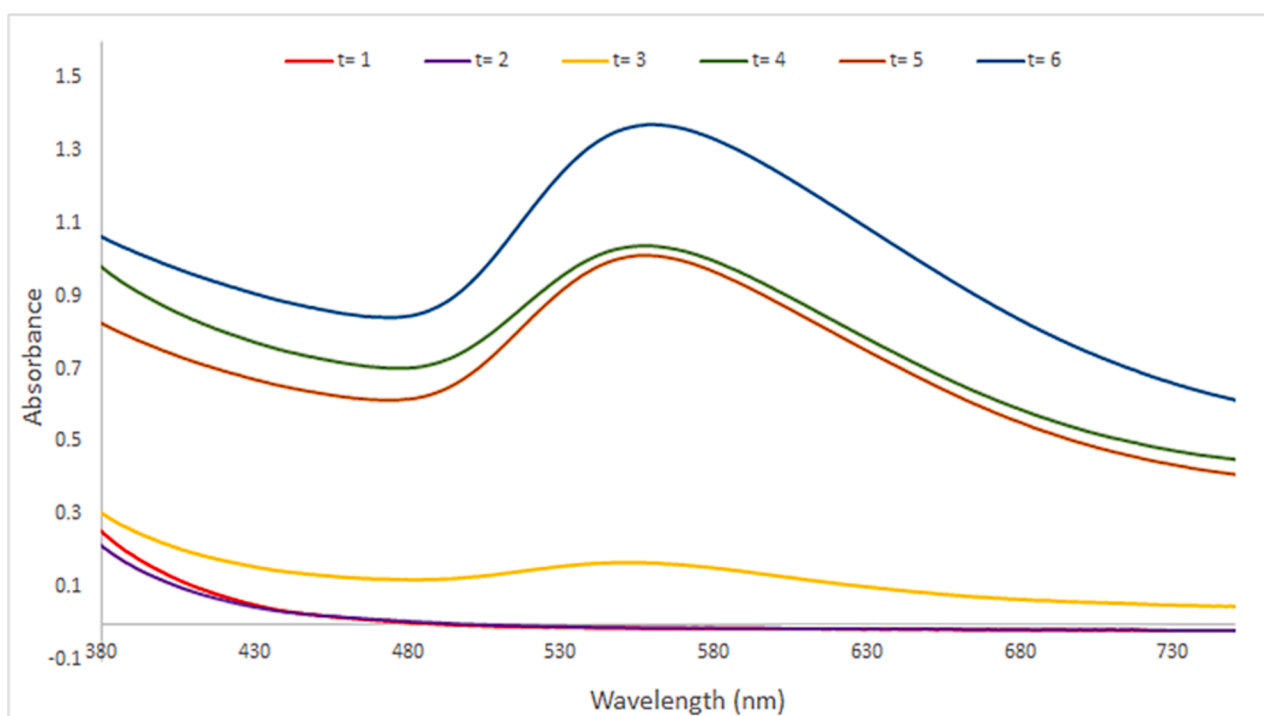


Fig. 3. UV-Vis absorption of (HAuCl₄·3H₂O) (1×10^{-3} M) (7 mL) with (2 mL) of *P. ligularis* extract after by varying the contact time (1–6)h at room temperature (25 °C..)

after that the peak intensity gradually decreases at 5 h, and finally it reaches a high absorbance at 6 h (Fig. 3). HRTEM images revealed identical outcomes that provided additional confirmation for the synthesized *P. ligularis*-AuNPs.

3.1.4. Effect of pH

The pH optimization of synthesized *P. ligularis*-AuNPs was achieved by conducting the reaction mixture at different levels of pH from pH= (1–6). The reaction used for the synthesis of *P. ligularis*-AuNPs was confirmed by UV–Vis absorption peak at a wavelength of 560 nm, where the peak strength increases with increasing pH from (1–3), but decreases at pH (4, 5, 6) (Fig. 4) (El-Naggar et al., 2016, Castro et al., 2018, Kang et al., 2018, Singh et al., 2018b, 2018a). It was clear from the plot that the strong SPR peak of the synthesized AuNPs was successfully obtained in acidic conditions, indicating fast synthesis. The results were further confirmed by HRTEM (Fig. 6) of the synthesized AuNP that were mostly homogenous particles at pH = 3, if the pH of the reaction was further increased the non-homogenous nanoparticles may be formed. In light of these observations, it can be concluded that pH = 3 (the usual pH of the extract solution) is the optimum pH for the synthesis of *P. ligularis*-AuNPs. The result was further reinforced by the HRTEM analysis that was shown in (Fig. 6).

3.1.5. Effect of temperature

The optimum temperatures used to synthesize *P. ligularis*-AuNPs were achieved by ranging the temperature from (15–35 °C) (Fig. 5). The observation of UV–Vis was carried out on the reaction mixture. The strength of the absorption peaks increased as the temperature of the reaction was increased up to (25 °C) and started to decrease at (30 °C), (35 °C). So, the optimum temperature for *P. ligularis*-AuNPs was at (25 °C) (Fig. 5) (Annamalai et al., 2013, Mohamed et al., 2014, Gnanaprakasam et al., 2016, Karthik et al., 2016, Castillo-Henríguez 2020). The *P. ligularis*-AuNPs synthesized were tiny, uniform, mostly spherical in shape, had a smooth surface, and did not form agglomerates.

3.2. EDX analysis

Further, the elemental illustrations were observed by energy dispersion X-ray analysis. The dry gold nanoparticles employed in the EDX examination showed a high-intensity typical signal at (1.8 keV) and (2.1 KeV) for Au metals and as well as other distinctive weak signals for phosphorus, calcium, and potassium (Fig. 7), that existed in the *P. ligularis*. Moreover, a significant carbon signal has been observed, which is thought to have been caused by the biomolecules present in the gold nanoparticles (Pham et al., 2011, Khan et al., 2018, Singh et al., 2018b, 2018a, Boomi et al., 2019, Ji et al., 2019).

3.3. X-ray diffraction analysis

The substance XRD was employed to examine the crystallinity and phase purity of AuNPs. Four peaks with diffraction angles of 38.1°, 44.51°, 64.61°, and 77.82° corresponding to the refractive index planes like (1 1 1), (200), (220), and (31 1) were detected in the XRD pattern. The results are consistent with those of previously reported literature that showed a characteristic pattern for AuNPs synthesized using a green synthesis technique (Gerald et al., 2016, Lee et al., 2016, Miri et al., 2018, Al-Radadi, 2021a,b). The average crystallite size for the synthesized AuNPs was measured by high-intensity (220) diffraction angles. Nonetheless, the peak intensity revealed that gold nanoparticles were crystalline in morphology (Fig. 8). The Debye-Scheerer formula was used to calculate the average crystallite size of synthesized nanoparticles.

$$D = \frac{K\lambda}{\beta \cos\theta}$$

Where Bragg's angle is denoted by symbol θ , the X-ray wavelength corresponds to λ that is (1.5406 Å), the full width at half maximum (FWHM) is represented by β , and D displayed the average particle size which was found to be in the range of 8.0 nm to 13 nm.

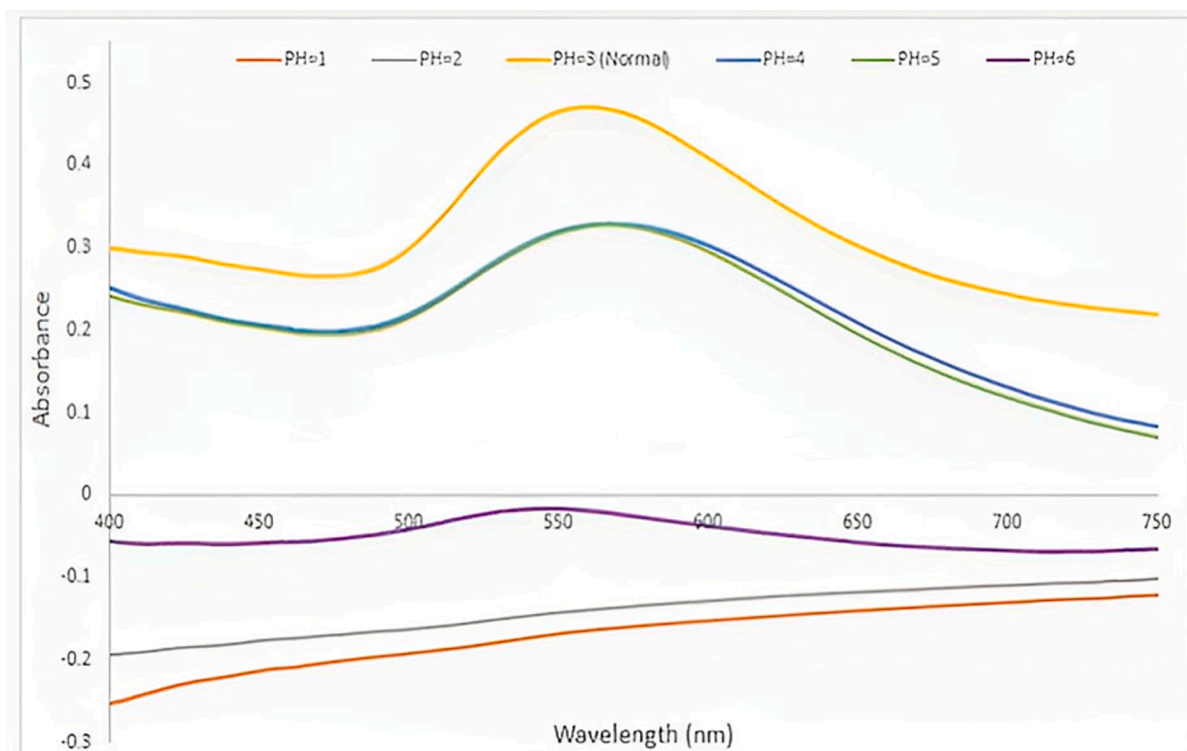


Fig. 4. UV–Vis absorption of (HAuCl₄·3H₂O) (1×10^{-3} M) (7 mL) with (2 mL) of *P. ligularis* extract after by varying the pH values (1–6), after 6 h at room temperature (25 °C..)

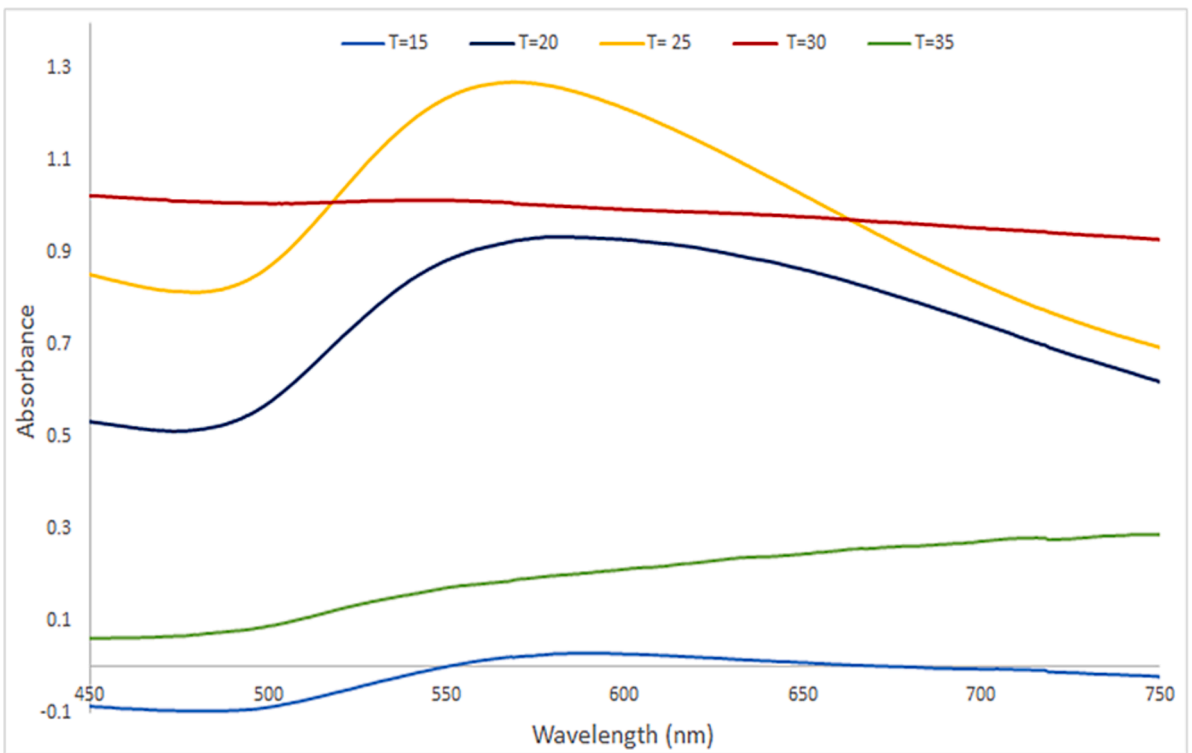


Fig. 5. UV-Vis absorption of (HAuCl₄·3H₂O) (1×10^{-3} M) (7 mL) with (2 mL) of *P. ligularis* extract at different temperature (15–35 °C), after 6 h of the reaction.

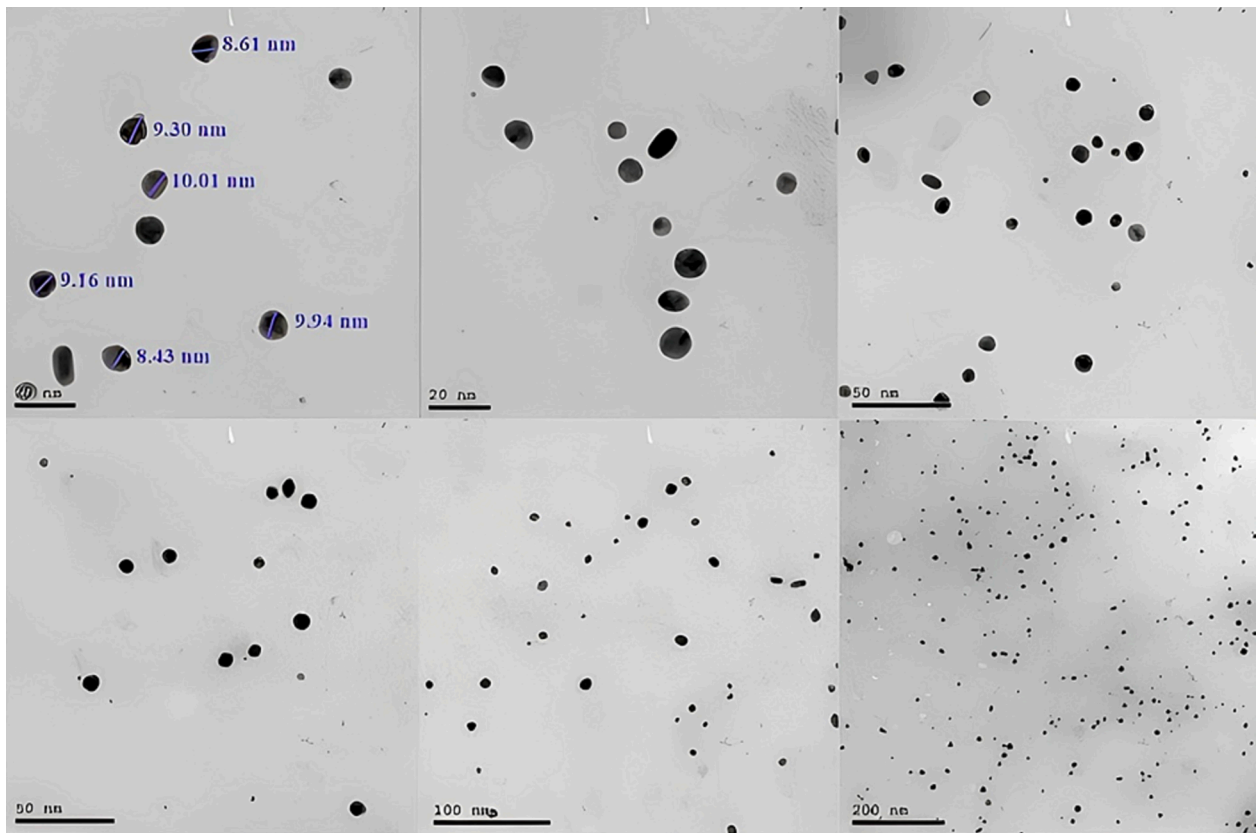


Fig. 6. HRTEM images of *P. ligularis*-AuNPs of *P. ligularis* (2 mL) with (7 mL) (HAuCl₄·3H₂O) (1×10^{-3} M) after 6 h at pH value (3), at 25 °C room temperature.

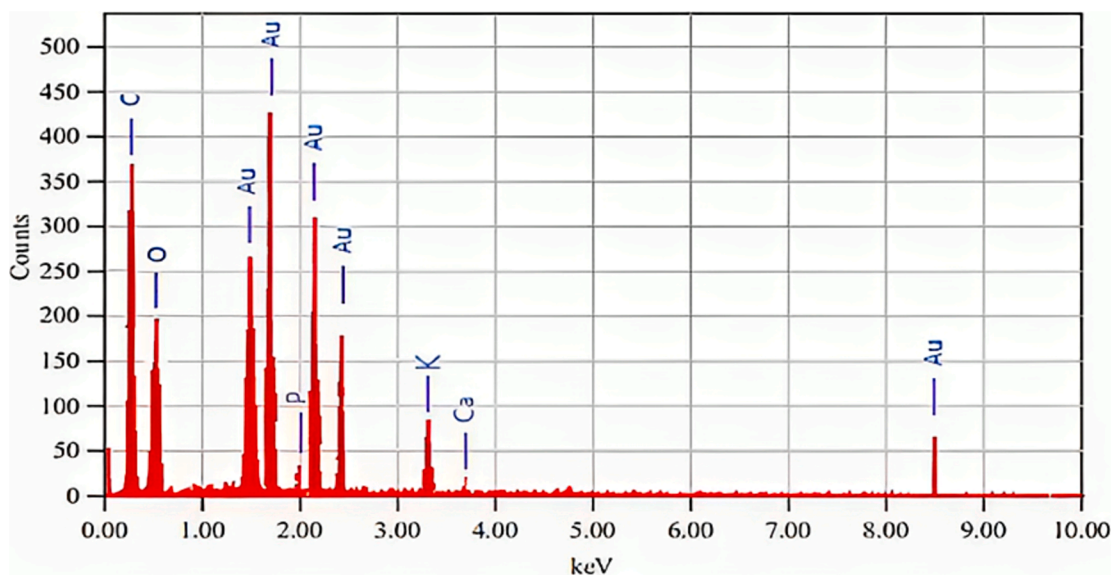


Fig. 7. EDX analysis for synthesized AuNPs.

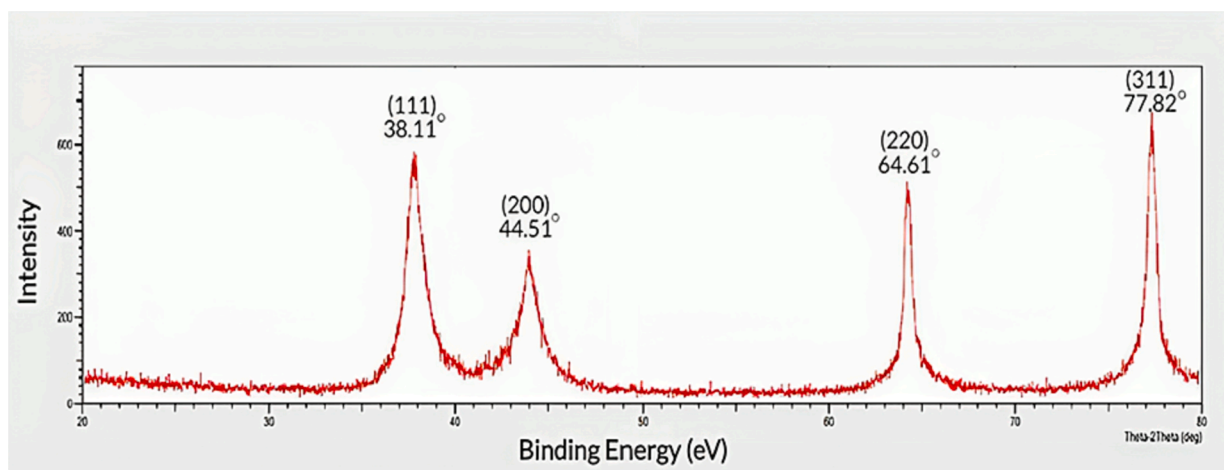


Fig. 8. X-ray diffraction pattern of *P. ligularis*-AuNPs.

3.4. High-Resolution transmission electron microscopic analysis

HRTEM images illustrate the size and morphological distribution of *P. ligularis*-AuNPs, as shown in (Fig. 6). The results revealed that the size of synthesized *P. ligularis*-AuNPs was in the range of 8.34 nm to 13 nm with non-aggregated spherical morphology. The dimension of *P. ligularis*-AuNPs was confirmed by the size distribution histogram analysis, which was shown in (Fig. 9A). The obtained data from the present investigation were consistent with the previously published report for AuNPs that showed compatible agreements. The zeta potential value of biogenic AuNPs was determined by sharp and signal peak obtained at -25.3 mV (Fig. 9B) (Ramakrishna et al., 2016, Hamelian et al., 2018, Vo et al., 2019).

3.5. Acute toxicity study

The acute toxicity test of these substances was investigated by applying various concentrations of *P. ligularis* extract and *P. ligularis*-AuNPs to rats. The extract of *P. ligularis* did not exhibit any obvious behavioral or morphological effects, such as hair loss, respiratory distress, convulsions, restlessness, coma, laxative use, urine, weight loss, or itching. The end of the treatment did not record any lethality at any of

the selected concentrations. The rats showed signs of tachycardia, increased respiration, and an arched back when exposed to AuNPs at a concentration of (8ppm) and no morbid, y or mortality was observed, even though such symptoms were hardly detectable at the dose (2ppm). Table 1

3.6. Effect of *p. Ligularis* and *p. ligularis*-AuNPs on neurobehavioral parameters

3.6.1. Reciprocal social interaction

The obtained data demonstrate the time of social interaction that was shorter in the autistic group of rats than in the Sham group ($p < 0.05$). In comparison, *P. ligularis* treatment improved the impairment in social interaction, and *P. ligularis*-AuNPs treatment reversed it (Amini et al., 2023) (Fig. 10).

3.6.2. Stereotypic behavior

The rats exposed to PPA exhibited more repetitive stereotyped behavior compared to the sham and ASD groups. Nonetheless, the amount of stereotypical behavior displayed by autistic rats was dramatically reduced after *P. ligularis* injection. The excessive repetition and stereotyping behavior were significantly reduced by *P. ligularis*-

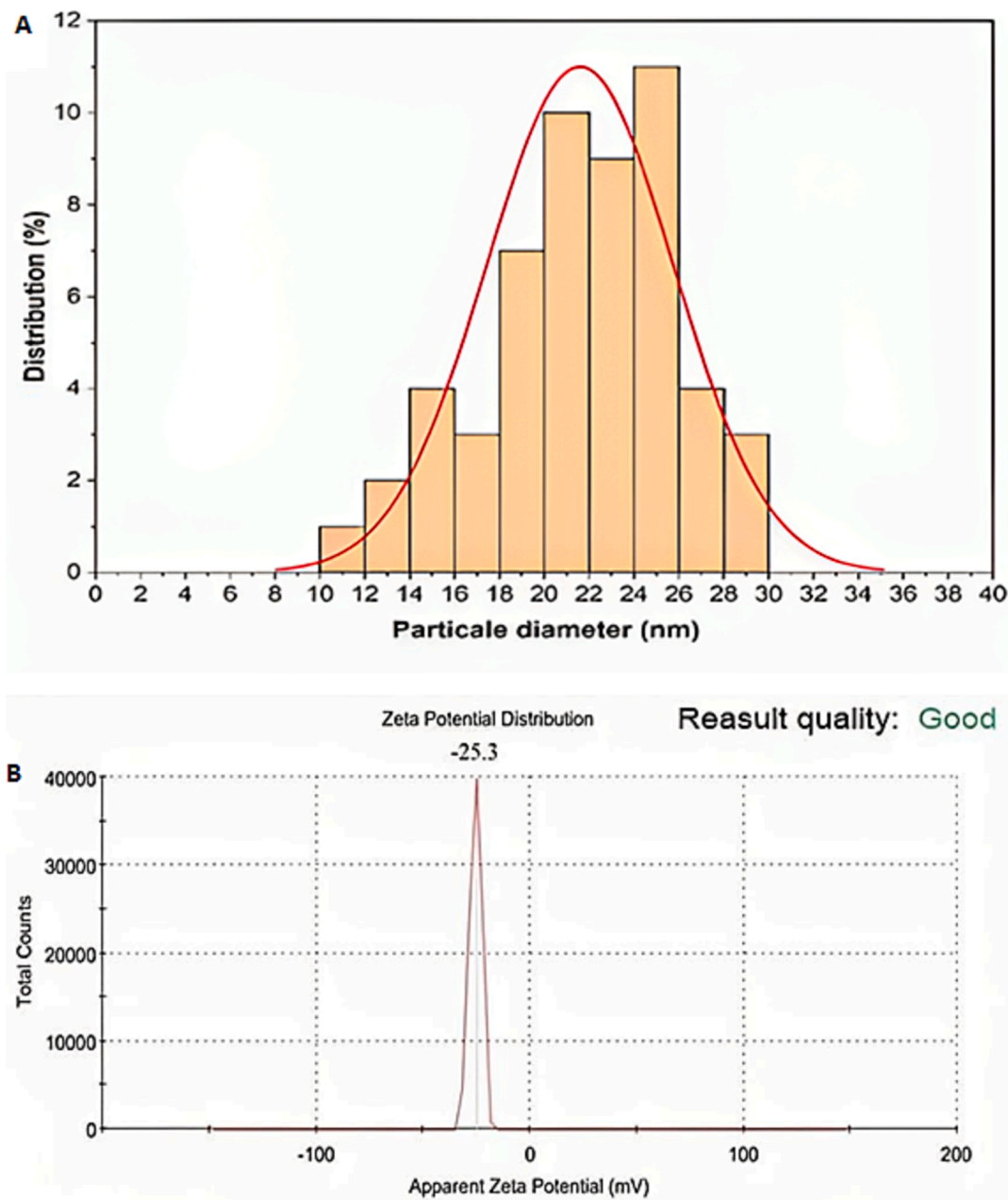


Fig. 9. Corresponding (A) size distribution graph and (B) Zeta potential of *P. ligularis*-AuNPs.

Table 1

Acute Toxicity results of synthesized AuNPs.

Samples	10 mg/kg	20 mg/kg	40 mg/kg
Control	19.3 ± 0.3	21.5 ± 0.4	23.7 ± 0.5
<i>P. ligularis</i>	18.2 ± 0.2	20.4 ± 0.3	22.5 ± 0.4
AuNPs	19.1 ± 0.3	23.7 ± 0.5	27.9 ± 0.5

AuNPs therapy ($p < 0.05$) (Abdelkader et al., 2022) (Fig. 11).

3.6.3. Elevated plus maze

The results demonstrated that PPA exposure significantly enhanced time spent in the closed arm while significantly decreasing time spent in the open arm in autistic rats as compared to the sham group ($p < 0.05$). Therefore, the treatment with *P. ligularis* or *P. ligularis*-AuNPs eases the abnormality that is caused by PPA which causes anxiety, however *P. ligularis*-AuNPs had a more pronounced effect than the *P. ligularis*

group (Anadozie et al., 2023) (Fig. 12).

3.6.4. Open field

The amount of time spent grooming and the amount of distance traveled increased significantly in induced PPA rats. Whereas the shorter rearing period in comparison to the sham group was observed as opposed to the ASD group. However, *P. ligularis* treatment improved these behavioral deficiencies. Moreover, treatment with *P. ligularis*-AuNPs reduced anxiety-related behavior ($p < 0.05$) (Abdelkader et al., 2022) (Fig. 13).

3.7. Effect of *p. Ligularis* and *p. ligularis*-AuNPs on biochemical parameters

3.7.1. Brain oxidative stress markers

The findings showed that the PPA-induced rats subsequently increased the MDA level in brain tissue (99.3 %), and those of SOD and

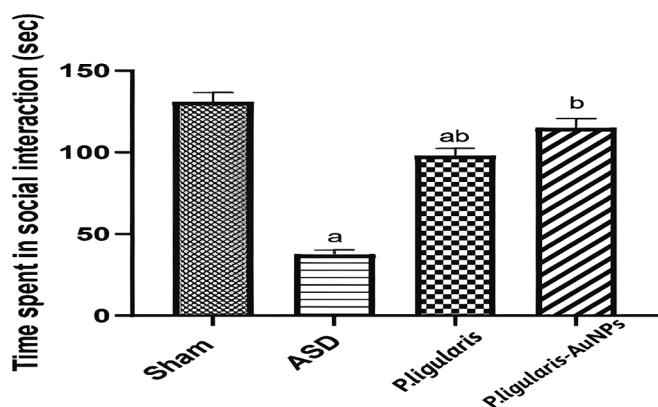


Fig. 10. Effect of AuNPs on PPA autistic rats behavioral parameters on reciprocal social interaction for 5 min.

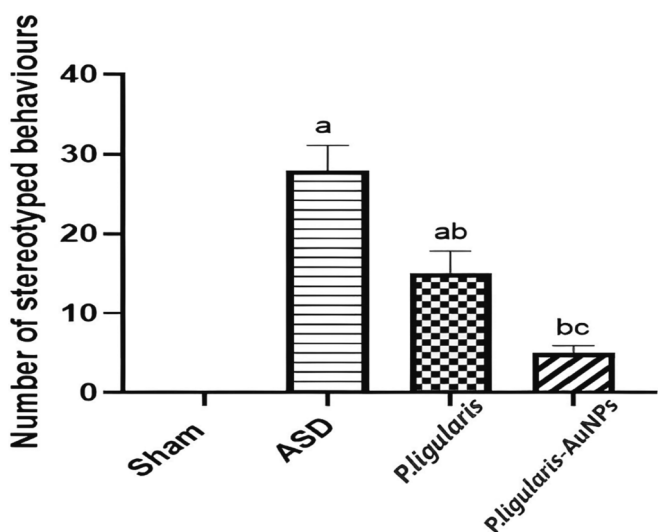


Fig. 11. Effect of AuNPs on PPA autistic rats on stereotype behavior test: repetitive, compulsive behavior was measured for 5 min.

GSH levels that were significantly depressed (-49.9 % and -82 %, respectively), in comparison to the sham group. The administration of *P. ligularis* considerably reduced oxidative stress markers, when compared to a group that had received PPA treatment. AuNPs treatment led to a significant restoration of oxidative stress markers in comparison

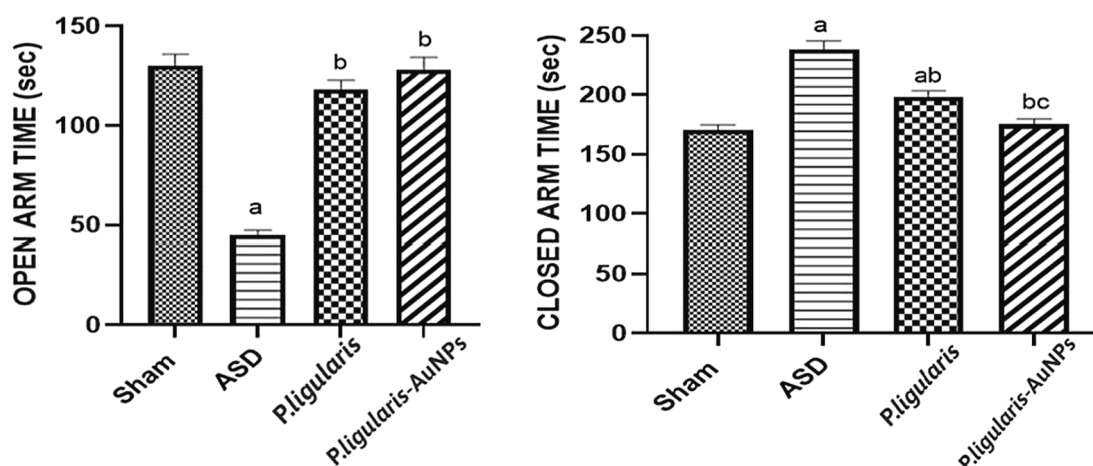


Fig. 12. Effect of AuNPs on PPA autistic rats behavioral parameters Elevated plus maze test: Time spent in opened and closed arm were assessed for 5 min.

to *P. ligularis* and the PPA group ($p < 0.05$) (Moldovan et al., 2022) (Fig. 14).

3.7.2. Brain inflammatory cytokines

According to the data, the PPA-treated group had a statistically significant increase in the IL-1 β and TNF- α levels in the brain (98.1 % and 170.7 %, respectively), in contrast to the sham group. The PPA-induced rat group along with *P. ligularis* demonstrated substantial increases in both IL-1 β and TNF- α levels (-33.6 %) and (-41.7 %), respectively. However, *P. ligularis* -AuNPs restored both brain IL-1 β and TNF- α ($p < 0.05$) (Sun et al., 2021) (Fig. 15).

3.7.3. Brain neurotransmitters

The PPA-induced ASD rats showed a substantial decrease in brain dopamine and serotonin (-74.2 % and -63.4 % respectively) associated with a significant elevation in brain glutamate level (124.1 %) versus the sham group. The treatment with *P. ligularis* induced observed a large increase in both serotonin and dopamine levels with a notable decrease in brain glutamate levels in brain in contrast to the PPA group. After the treatment of *P. ligularis*-AuNPs subsequent increases in brain dopamine and serotonin are shown, whereas glutamate levels were brought back to normal in comparison to the PPA-induced ASD group (Jawna-Zboińska et al., 2016) (Fig. 16).

3.7.4. Neurochemical parameters

The results demonstrate that PPA injection enhances the brain ERK (Tiwari et al., 2021) and MBP (Khera et al., 2022) (186.4 % and 67.6 %, respectively). The administration of *P. ligularis* significantly decreased both ERK and MBP in contrast to the PPA group. The *P. ligularis*-AuNPs showed maximum restoration of ERK and MBP levels in contrast to the PPA group and surpassed by *P. ligularis* in autistic rats ($p < 0.05$) (Fig. 17).

3.8. Effect of *p. Ligularis* and *p. ligularis*-AuNPs on molecular parameters

3.8.1. Apoptotic genes analysis

When rats exposed to PPA had significantly upregulated the apoptosis-related genes level of the caspase-3 (150.5 %) and bax (170 %), compared to the sham group, while Bcl2 expression was significantly downregulated (-49.6 %). The analysis of apoptotic genes was remarkably improved by the administration of *P. ligularis*, and was almost normalized by the treatment of *P. ligularis*-AuNPs ($p < 0.05$) (Sato et al., 2022) (Fig. 18).

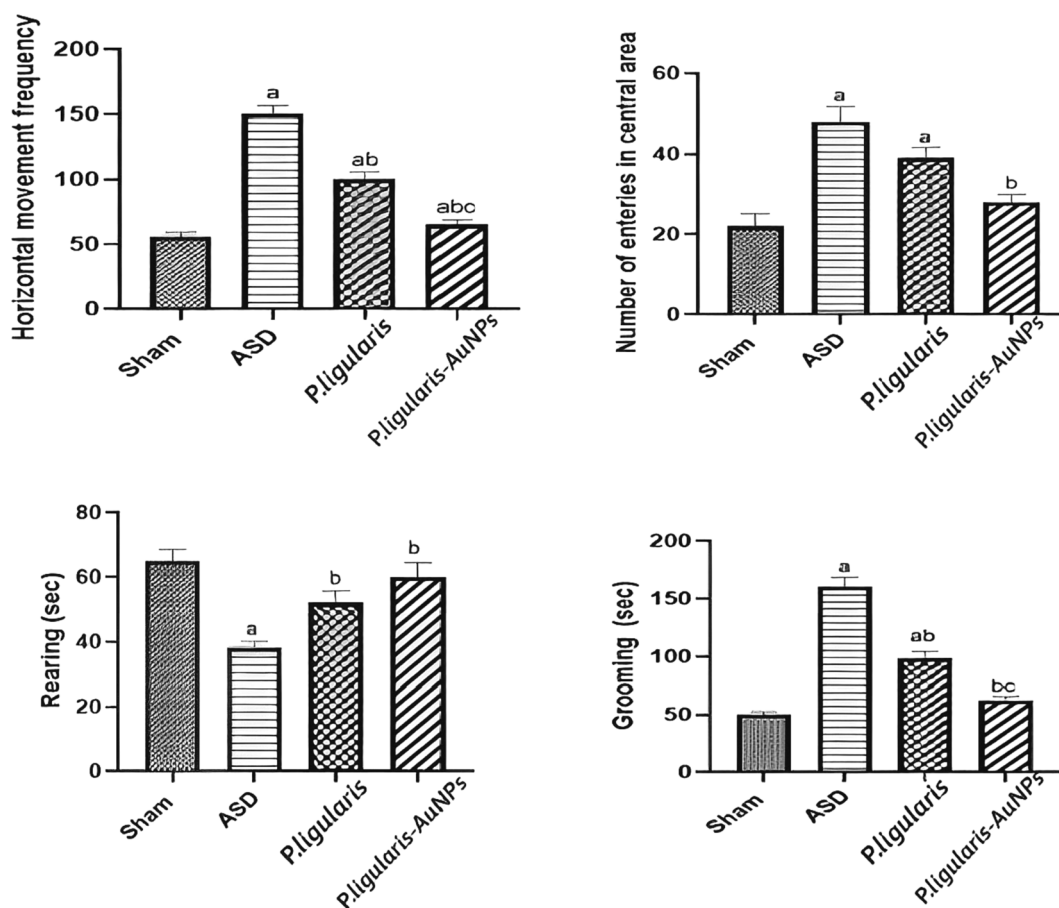


Fig. 13. Effect of AuNPs on PPA autistic rats behavioral parameters.

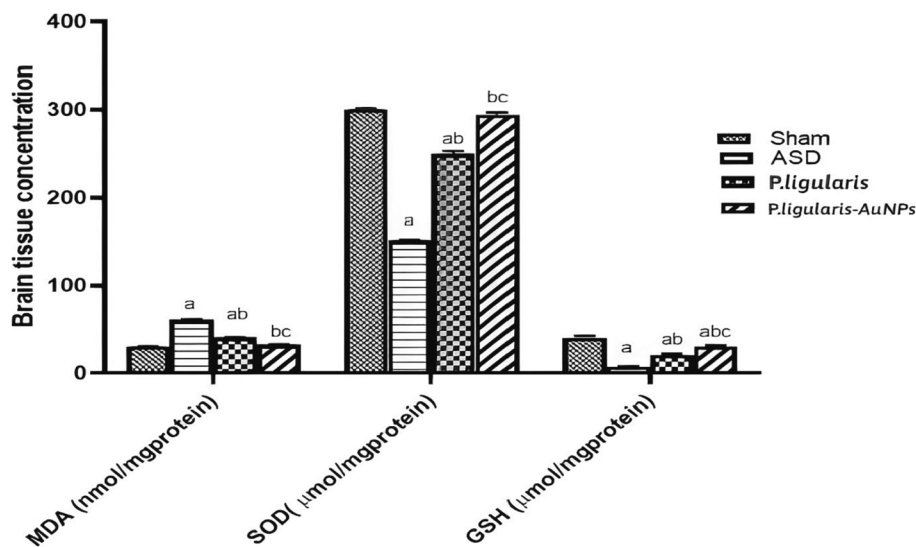


Fig. 14. Effect of AuNPs on PPA autistic rats oxidative stress markers: superoxide dismutase (SOD), brain Malondialdehyde (MDA), and reduced glutathione (GSH).

3.9. Histopathological investigation

According to histopathological evaluation of the tissues, the PPA injection caused several areas of necrosis in the tissues of rat brain, which were surrounded by rims of astrocytic reaction that were noticeably congested and areas of vacuolar degeneration (Doğan et al., 2023). When autistic rats were treated with *P. ligularis*, there was a marginal improvement in the brain tissues compared to the PPA group, but

continuous astrocytes, necrosis, no degeneration, and less congestion were examined. The rats treated with *P. ligularis*-AuNPs indicated that the brain tissues had significantly improved, as evidenced by an astrocytic reaction, less necrosis, no degeneration, and minor congestion were observed in the brain tissues (Fig. 19).

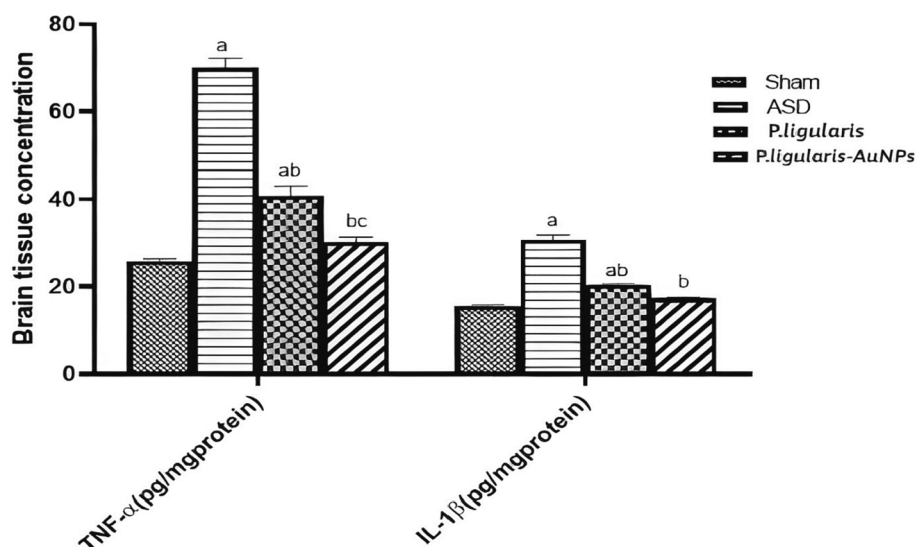


Fig. 15. Effect of AuNPs on PPA autistic rats' Inflammatory cytokines: interleukin 1 beta (IL-1 β), and brain tumor necrosis alpha (TNF- α).

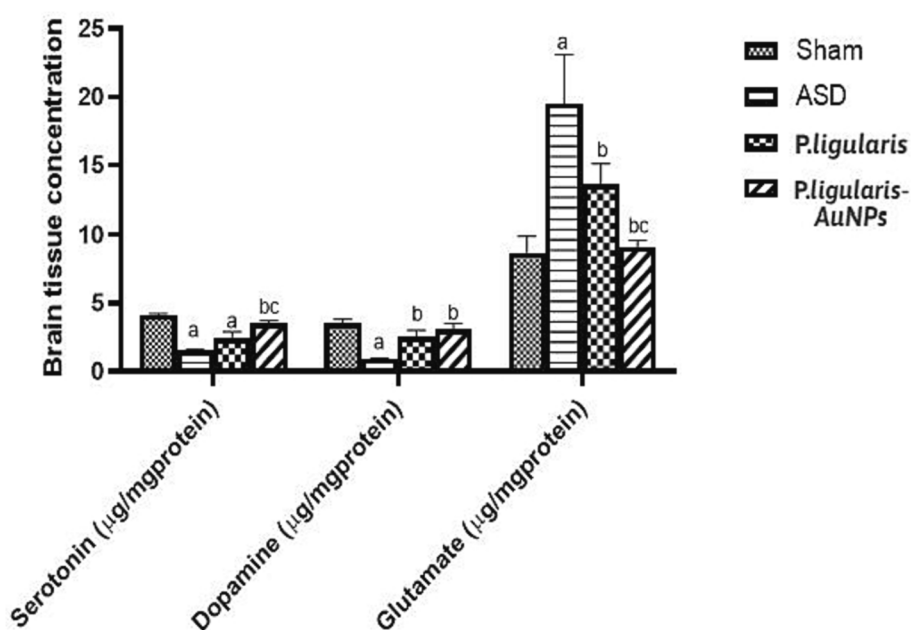


Fig. 16. Effect of AuNPs on PPA autistic rats brain neurotransmitters: serotonin, dopamine, and glutamate.

4. Discussion

The current investigation aimed to synthesize plant-based synthesis of AuNPs using *P. Ligularis* plant extracts that were responsible for the reduction of (HAuCl₄·3H₂O) and act as stabilizing and capping agents. The *P. ligularis*-AuNPs were characterized by different spectroscopic techniques and were then employed for investigations into the biological potential. The different parameters of reaction were used to optimize *P. ligularis*-AuNPs for instance the volume of *P. ligularis* plant extract, volume of metal ion (1×10^{-3} M) (HAuCl₄·3H₂O), temperature, pH and reaction time (Al-Radadi, 2022a). According to the results, the best volume for a metal ion (1×10^{-3} M) (HAuCl₄·3H₂O) was found to be (7 mL) and the specified effective volume of *P. ligularis* extract was 2 mL, that was supported by UV-Vis and HRTEM research. The low intensity peak gradually increased as the extract volume went from 1 mL to 3 mL. Similarly, the (1×10^{-3} M) (HAuCl₄·3H₂O) volume increased from (1–8 mL) and also showed significant intensity augmentation from

556 nm to 559 nm peaks in UV-Vis absorption. The result demonstrates that the small volume (5 mL) (HAuCl₄·3H₂O) solution showed a small peak intensity at a wavelength of 556 nm. In addition, when the volume was increased to (7 mL), the UV-Vis absorption displayed the highest peak intensity and a strong SPR (surface plasmon resonance) absorption peak at a wavelength of ($\lambda_{max} = 559$ nm). The volume was further increased up to (8 mL) the peak intensity shifted towards the red area (bathochromic) at a wavelength of (566 nm), indicating that the optimum volume is (7 mL) (Fig. 2) (Milaneze et al., 2014), Jafarizad et al., 2015, Wahab et al., 2018, Latha et al., 2019, Sunayana et al., 2020). Similar findings from the HRTEM analysis revealed that AuNPs were an identical in size and shape without aggregation.

The visible spectra of *P. ligularis*-AuNPs were examined for the distinct peak at max = 559 nm that attribute to metallic nanoscale gold and is related to the synthesis of AuNPs (Ismail et al., 2018). It is confirmed by studying HRTEM visuals, as the synthesized *P. ligularis*-AuNPs attained a spherical shape and were distributed evenly with no

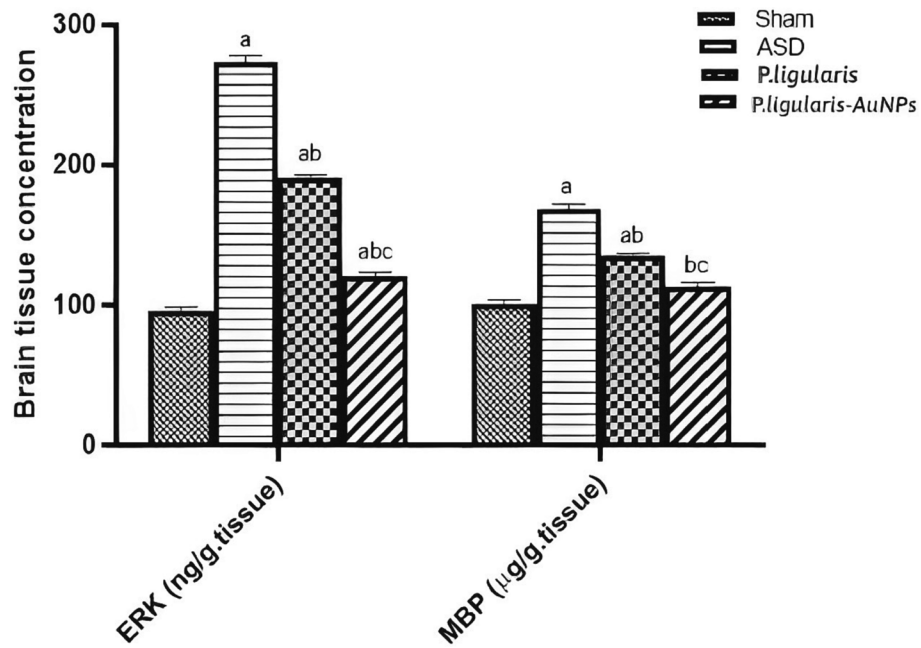


Fig. 17. Effect of AuNPs on PPA autistic rats brain neurochemicals: Myelin basic protein (MBP), and extracellular signal-regulated protein kinase (ERK).

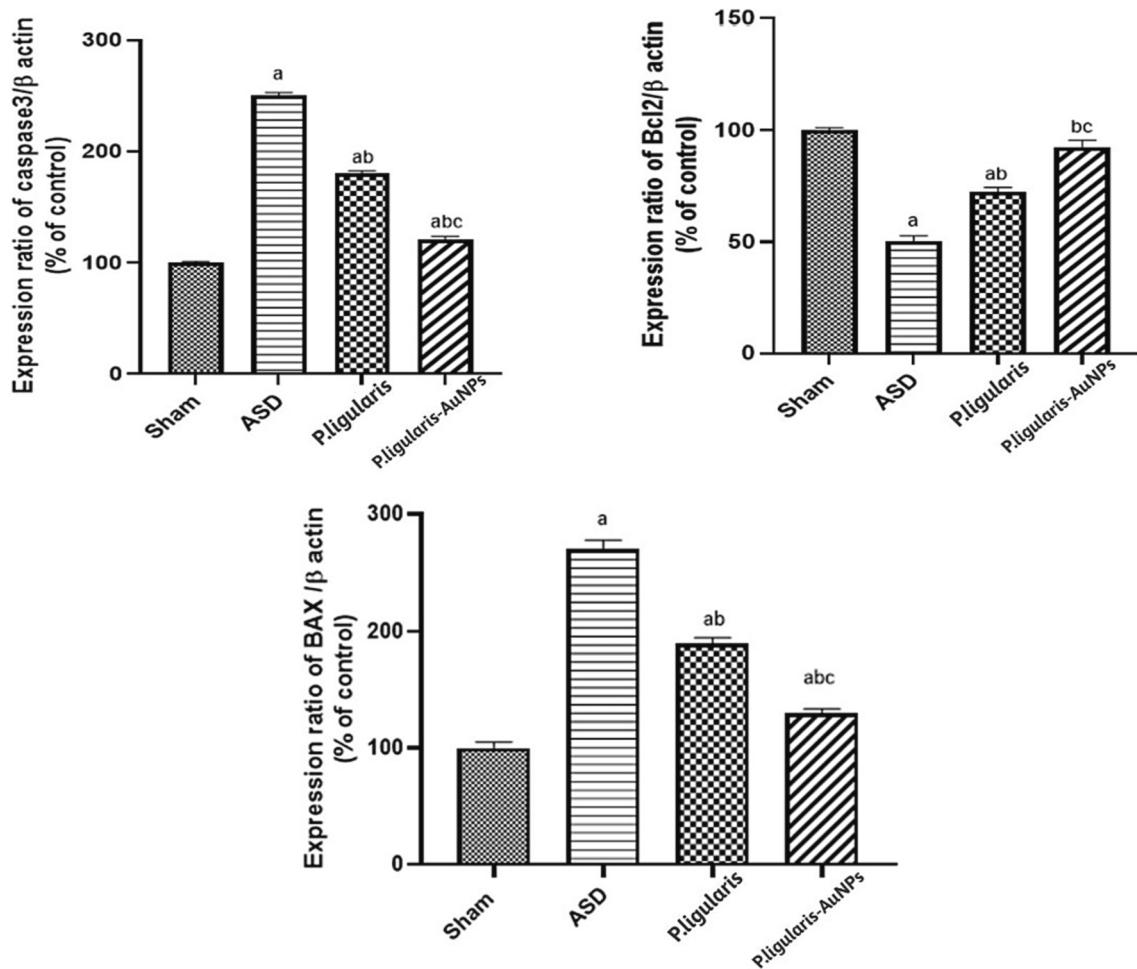


Fig. 18. Effect of AuNPs on PPA autistic rats apoptotic genes expression in mRNA caspase-3, Bax, B-cell lymphoma 2 (Bcl2).

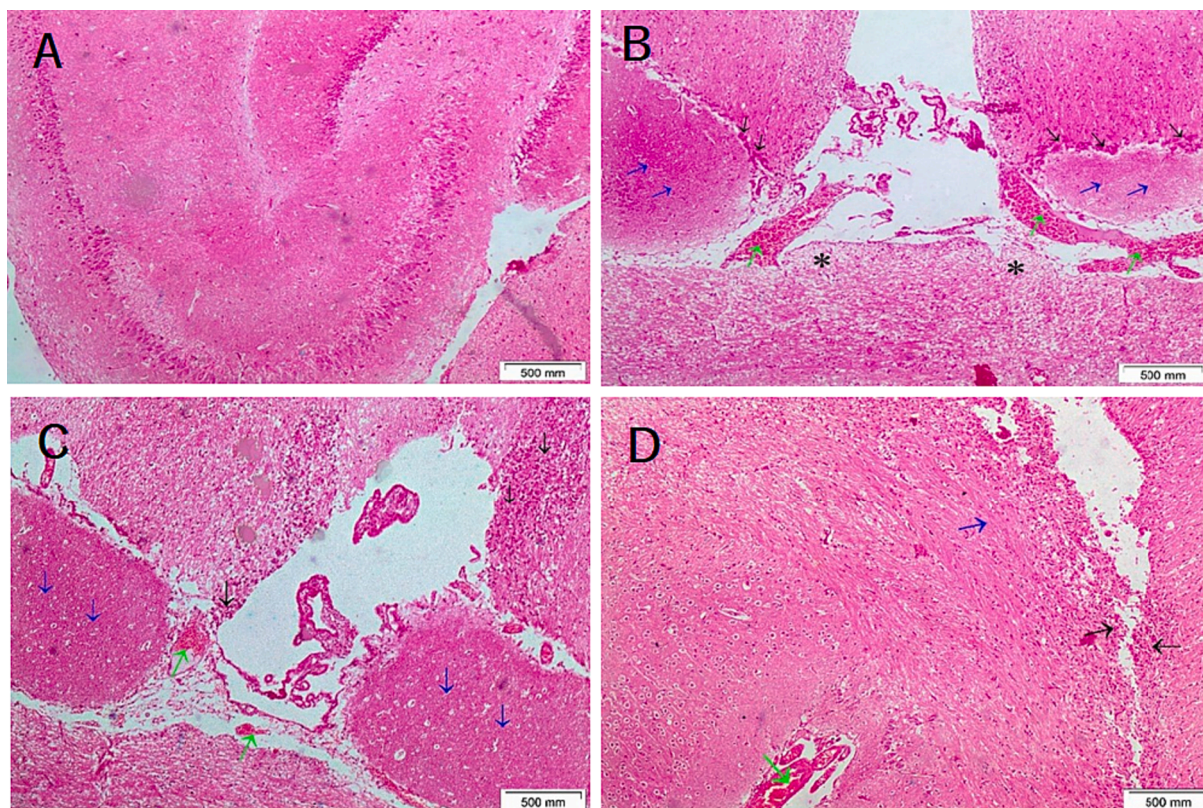


Fig. 19. Photomicrographs of rat hippocampal tissues.

aggregation (Fig. 6). The *P. ligularis*-AuNPs were recognized spherical with polydisperse results with a high SPR peak in the spectra (Sunayana et al., 2020). One of the most important factors that determined the size of *P. ligularis*-AuNPs was contact time that revealed high-intensity absorption peak with (2 mL) sweet granadilla extract and (7 mL) (1×10^{-3} M) ($\text{HAuCl}_4 \cdot 3\text{H}_2\text{O}$) at room temperature and up to 6 h, as shown in (Fig. 3). As the period expanded, the colour change was observed for the stable synthesis of *P. ligularis*-AuNPs. Since the peak amplitude was proportional to the contact time, it also increased as time passed. The plot illustrated that the absorption of the peaks increased sharply up to 4 h and then slowed and decreased at 5 h after that it showed high absorbance and optimum results were obtained at 6 h (Murad et al., 2018).

Furthermore, the synthesis of *P. ligularis*-AuNPs examinations were conducted at various temperatures (15–35 °C) (Fig. 5). The data revealed a broad absorption peak at 15 °C, but upon increasing the temperature of the reaction from 20 °C to 25 °C, a sharp peak of intensity appeared. It is implied that there is no reaction occurring at 15 °C and that no distinctive AuNPs peak forms. However, as the reaction temperature increased from (30 °C) to (35 °C), the peak intensity reduced. As a result, 25 °C is thought to be the optimum temperature of the reaction for the synthesis of *P. ligularis*-AuNPs (Gnanaprakasam et al., 2016).

Moreover, the optimum pH used for the synthesis of AuNPs was to change the pH conditions of the reaction. The pH range was 1–6 where the results suggested that the peak intensity is increased upon increasing the pH from (1–3), nothing happened when the reaction continue up to pH 3. Interestingly, the product displayed a strong characteristic peak (max = 559 nm) at pH 3, indicating that the pH level was suitable for the product's formation. The peak broadening may be caused by the reaction molecules being hampered by hydrogen bonding interactions with the functional groups present in the constituents of *P. ligularis* plant extract, whereas the decreased intensity indicates that the reactions are inactive (Castro et al., 2018). The results that were obtained were

consistent with previous investigations, that described that *Ephedra* plant extract was used to reduce AuNPs under various conditions, including volume, pH, temperature, and reaction time (Al-Radadi, 2023).

The HRTEM images of *P. ligularis*-AuNPs showed spherical shape with particle size ranges 8.34 nm to 13 nm. This might be owing to the accessibility of various components in plant extract that act as capping agents. Similar results were reported earlier for *P. ligularis*-AuNPs that are consistent with the current study (Vo et al., 2019). Further, the potential difference between the dispersion medium and the stationary layer of fluid associated with the dispersed particle was verified by the zeta potential (ZP), which offers information on the surface charge of nanoparticles. ZP is an essential asset using *P. ligularis* to assess the stability and surface charge of the Au-NPs. The biogenic *P. ligularis*-AuNPs showed exceptional stability at 25 °C and the ability to prevent aggregation due to their negative surface charge due to negative surface charge that was -25.3 mV (Fig. 9(B)) (Balasubramanian et al., 2020; Al-radadi, 2023).

The crystal structure and phase of *P. ligularis*-AuNPs were identified using X-ray diffraction patterns. The four peaks obtained from the XRD analysis were related to the (111), (200), (220), and (311) planes with diffraction angles of 38.1°, 44.51°, 64.61°, and 77.82° corroborated the phase purity and were in good agreement with previously published data. The Debye-Scherrer equation was used to determine the mean size of nanoparticles that was in the range of 8.0 nm to 12.513 nm for Au NPs and were consistent with the TEM results (Fig. 6) 8.34 nm to 13 nm (Miri et al., 2018, Al-Radadi, 2021). Additionally, the elemental composition of synthesized nanoparticles were determined by EDX analysis. It facilitates the presence of gold, carbon, oxygen, calcium, potassium, and phosphorus spots, which provides more evidence in favor of the coordination of organic substances (phytochemicals) with metal atoms to produce *P. ligularis*-AuNPs (Khan et al., 2018, Boomi et al., 2019).

Autism spectrum disorder (ASD) is characterized by behavioral, memory cytoarchitecture, and intellectual deficits and is one of the most

prevalent neurocognitive disorders. The present study investigated the neuroprotective effect of *P. ligularis* extract and *P. ligularis*-AuNPs in PPA-induced autism in rats. The behavioral tests were conducted as well as oxidative stress, anti-inflammatory, neurotransmitter, neurochemical, and molecular markers in the homogenate brain of rats were assessed. In addition, histopathological alterations in brain tissues were investigated. PPA-induced autism is a well-established experimental animal model of autism that can induce neurobehavioral impairment (Mirza and Sharma, 2019, Doğan et al., 2023).

In this study, rats exposed to PPA exhibited autistic-like phenotype and behavior, which was shown by a decrease in the amount of time spent performing social interaction and an increase in stereotyped/repetitive behavior and grooming. Furthermore, PPA-induced rats demonstrated anxiety-related behavior in open field, elevated plus maze, and rearing time tests. The aforementioned findings were in agreement with earlier research using the ICV PPA rat model (Lobzhanidze et al., 2020). The biochemical effects of propionic acid, induced change in the neural function, increased NMDA receptor sensitivity, inhibited $\text{Na}^+/\text{K}^+ + \text{ATPase}$, elevated nitric oxide, and promoted intracellular calcium release, all have the potential to change neurotransmission in different parts of the brain and be the source of these behavioral deficits (Quednow et al., 2004). Moreover, weak acid propionic acid has the potential to gradually accumulate in CNS cells, increasing intracellular acidosis, disrupting synaptic transmission and other neuronal functions, and ultimately causing behavioral and neurological abnormalities (Tannock and Hot, 1989, Mehan et al., 2020).

Neurological disorders have a direct relationship with oxidative stress and neuroinflammation (Salem et al., 2016, Alesawy et al., 2021) and are essential to the development of autism. Our findings showed that PPA-induced polyunsaturated fatty acid oxidation produced MDA, which causes biomolecular damage and inhibited the level of antioxidants in brain tissue. According to the investigation, MDA levels increased in blood samples from a patient with autism spectrum disorders because of oxidative stress (González-Fraguela et al., 2013). Another study revealed that MDA levels were also elevated in ASD, suggesting that these patients may be more susceptible to oxidative stress due to the immaturity of their antioxidant responses (Zoroglu et al., 2004, Meguid et al., 2011). These findings suggested that the autistic brain may be more susceptible to oxidative stress.

By certain investigations, CNS-specific inflammation may be involved in the development of ASD (Vargas et al., 2005, Zimmerman et al., 2005). The data clearly showed an increase in $\text{IL-1}\beta$ and $\text{TNF-}\alpha$ in the brain homogenates of PPA-treated rats, suggesting a role for PPA in neurotoxicity. These results are consistent with those of several clinical investigations on the cytokines in the brains of autistic patients (Li et al., 2009, Ashwood et al., 2011, Sun et al., 2021). It was observed that proinflammatory cytokines, chemokine (IL-8), and Th1 cytokines levels remained high in the patients of ASD, indicating that PA may still have a role in the etiology of autistic symptoms. Moreover, it was also shown that brain tissues of rats administered intracerebroventricular PPA injections had spectacular reactive astrogliosis and microglia activation, presenting evidence of an intrinsic neuroinflammatory response (Shultz et al., 2011).

Brains of individuals with autism have been reported to suffer from neurotransmission disruption which alters inhibition in the brain network and affects the ability to perceive emotional expressions (Oblak et al., 2011). The present investigation discovered that brain homogenates from PPA-treated rats had significantly lower levels of serotonin and dopamine as well as notably higher levels of glutamate. These findings are in agreement with previously reported literature (Azmitia et al., 2011) where the decrease in serotonin transporter activity and tryptophan retention in autistic patients were observed. Also, the decrease in dopamine levels observed in this study was similar to previous investigations (Garnier et al., 1986, Mandic-Maravic et al., 2022), which found elevated levels of homovanillic acid (HVA) and dopamine

hydroxylase in autistic children which contributes to development of autistic signs. The increase in Glu activates glutamate receptors, that might induce excitotoxicity and cause the death of neuronal cells. Glu is speculated to have important effects in several forms of neurodegeneration, because of the potential for leakage from damaged tissues. Glu excitotoxicity is generally triggered by microglial activation and excessive stimulation of Glu receptors, which has been linked to PPA neurotoxicity as well as impaired brain development and synaptic plasticity (Flores-Méndez et al., 2016, El-Ansary et al., 2017).

The development of neurons and the activation of the adult brain can both be significantly influenced by ERK. ERK1 and ERK2 have important roles in the regulation of adult nervous functional units, including learning, neuroinflammation, memory formation, synaptic plasticity, and neuronal death (Sun and Nan, 2017). The pathogenesis of the neurological condition associated with ASD is characterized by abnormal ERK signaling. Several ERK inhibitors have shown promising results in curing a wide range of ailments, including brain injuries (Mori et al., 2002), Parkinsonism (Quesada et al., 2008), autoimmune disease (Breton et al., 2009), and ASD (Yufune et al., 2015). According to recent data, PPA-induced ASD in rats significantly increased the ERK levels. These findings support a prior study that claimed ERK hyperactivation was responsible for the development of CNS pathologies in the autoimmune ASD animal model (Albert-Gascó et al., 2020). Our findings showed that after PPA administration, MBP was significantly increased. MBP is a structural protein required for the formation of the myelin sheath and helps in the proliferation of neural stem cells during neurogenesis, which is a significant pathological feature of ASD (Mirza and Sharma, 2019). According to previously reported literature (Khanbabaei et al., 2019), both male and female autistic mice had enhanced myelination in their frontal brains, which was associated with higher levels of myelin basic protein. When apoptotic gene expression was examined in autistic rats, it was observed that Bax (a pro-apoptotic marker), and caspase-3 (an apoptotic marker) gene expression were significantly upregulated, while Bcl2 (an anti-apoptotic marker) expression was downregulated. Recently, similar reports were available on a challenge that arises in apoptotic markers together with evidence of an increase in caspase-3 in autistic rat brains due to BBB disruption, apoptosis, and/or neurodegeneration, which are PPA neurotoxic indicators (Olczak et al., 2010).

The histopathological analysis of the brain tissues of the PPA-treated rats showed several areas of necrosis surrounded by a demarcating rim of astrocytic response, with congestion and areas of vacuolar degeneration which confirms the assertion that PPA is neurotoxic (Doğan et al., 2023).

On the other hand, the present investigation demonstrated that treating rats with *P. ligularis* extract considerably improved the parameters. Significantly, the treatment of *P. ligularis*-AuNPs restored these values to the range that was considered normal. The existence of various major biomolecules, such as alkaloids, flavonoids, cyanogenic, phenols group, minerals, vitamins, glycosides, and terpenoid compounds, distinguishes *Passiflora* species from other plants (Zibadi and Watson, 2004). The anti-anxiety activity of *P. ligularis* extract may have contributed to the improvement of behavioral impairments observed during this investigation after *P. ligularis* extract administration (Coleta et al., 2001) stated that the open field, horizontal-wire, and elevated plus mazes tests on rats were used to explore the anti-anxiety activity of *P. ligularis*. The aqueous extract had anxiolytic-like properties without having a large impact on neuronal activity.

P. ligularis is abundant in polyphenols and has been considered a natural antioxidant. The findings showed that *P. ligularis* administration decreased MDA levels and increased SOD and GSH in the brain tissues of autistic rats. Other study report the antioxidant activity of *P. ligularis* which was concentration-dependent, and was tested against DPPH radical and several reactive oxygen species (superoxide radical, hydroxyl radical, and hypochlorous acid) (Zeraik et al., 2011). The neutrophil peroxidase activity as well as the myeloperoxidase enzyme

present in neutrophil granules were reported to be inhibited by *P. ligularis*. Additionally, the maintenance of SOD and GSH levels enhances the antioxidant capacity of *P. ligularis* and contributes to its protective effect against neurological disorders.

On the other hand, TNF- α and IL-1 β levels were markedly reduced after the administration of *P. ligularis*. These findings were consistent with those of (Benincá et al., 2007), which state that the *Passiflora* species aqueous leaf extract demonstrated potential anti-inflammatory in the *in vivo* experimental model hindered pleural cavity of leukocyte influx that was linked with an obvious blockade of nitric oxide, myeloperoxidase, cancer, interleukin-1 levels, and cell necrosis factors in the acute model of inflammation caused by intrapleural injection of rats. Dexamethasone was less effective than *P. ligularis* at reducing the levels of interleukin-1 and tumor necrosis (Capasso and Sorrentino, 2005).

The current data showed that consumption of *P. ligularis* greatly reduced the disruption of neurotransmitters, which was demonstrated by an increase in serotonin and dopamine levels and a decrease in glutamate levels. These results were consistent with (Jawna-Zbojńska et al., 2016), who showed that groups receiving *P. ligularis* extract exhibited a glutamic acid reduction. The main excitatory neurotransmitter is glutamic acid, which also serves as a source of the inhibitory neurotransmitter GABA. The most crucial CNS controlling mechanism is the balance between these two systems (Zhou and Danbolt, 2014). Presynaptic GABAA receptor activation inhibits glutamate release by lowering the calcium ion influx carried on by depolarization. The basic consequence of damaged brain neurons is the release of excessive glutamic acid, which causes excitotoxicity and alterations in GABA release (Waldmeier et al., 2008). Glutamic acid/GABA system imbalance is a significant contributing factor to many CNS disorders, including depression, anxiety, epilepsy, and addiction. The activation of GABAA and GABAB receptors may have a neuroprotective effect. The anxiety-reducing effect results from stimulating GABAA receptors (Guerrini et al., 2013). Therefore, the release of DA is inhibited by glutamate through the action of AMPA receptors. On the other hand, the stimulation of the GABAA receptor opposes the mechanism and promotes the release of DA (Avshalumov et al., 2003). Furthermore, the inflammatory cytokines and inflammatory responses are elaborated in the ASD transmission. *P. ligularis*'s ability to reduce inflammation may be a viable mechanism by which it improves neurological impairment and increases levels of serotonin and dopamine.

MAPKs, a group of signaling molecules that includes the proteins ERK, p38, and JNK, probably play a significant role in the mechanisms that cause inflammation (Lasa et al., 2002). According to current information, plant *P. ligularis* treatment significantly reduced ERK levels in brain homogenate. Similar findings from a prior study showed that LPS-induced ERK, p38, and JNK phosphorylation were substantially blocked when *P. ligularis* was used as a medication. The *P. ligularis* exhibited promising MAPK pathway inhibition. The inhibition of the main MAPK signal in the basic inflammatory response is affected by related disorders (Cañas et al., 2010). The primary myelin protein, myelin basic protein (MBP) translations are regulated efficiently by ERK, which in turn controls the timing of remyelination (Michel et al., 2015). That explains why MBP decreased in autistic rats which administered *P. ligularis* treatment.

In autistic rats, *P. ligularis* extract administration demonstrated a neuroprotective effect against PPA-induced apoptosis. Significant downregulation was observed in Bax and caspase-3 expression along with an elevation in Bcl2 expression. These findings were in agreement with another earlier research (Fu et al., 2016, Wen et al., 2018). They showed that *P. ligularis* inhibited apoptosis mediating the PI3K/Akt/Bad signalling and downstream mitochondria-caspase-3-dependent cell death pathway in PC12 cells. Moreover, *P. ligularis* reduced intracellular ROS generation in rat primary cortical neurons via the PI3K/Akt signaling pathway to prevent neurotoxicity.

Importantly, *P. ligularis*-AuNPs accomplished better effects than *P. ligularis* extract in all of the variables examined. This finding may be

explained by the functional groups found in plant extracts and the morphological identities of AuNPs, where biomolecules act as a stabilizing agent that can employ their influence to the benefit of nanoparticle aggregation. These results are consistent with the research of (Boruah et al., 2021), which examined the green synthesis of AuNPs using *P. ligularis*. It was found that green AuNPs synthesized by *P. ligularis* extract exhibit greater antioxidant activity, lower toxicity, and assist in the regeneration of neuronal cells in animal models. It demonstrates that integrating various plant extract fractions to stabilize AuNPs may be the driving force behind the increase in the bioactive nature of green AuNPs. Moreover, histopathological investigation in the current study indicated that brain sections of *P. ligularis*-treated rats showed areas of necrosis, and astrocytic reaction, with mild congestion. In *P. ligularis*-AuNPs-treated rats, brain sections showed less tissue damage, and fewer lesions were observed to be decreased and closer to normal tissue.

5. Conclusion

The current study established a simple and direct, environmentally friendly, energy-saving, and cost-effective approach used for the successful synthesis of *P. ligularis*-AuNPs by sweet granadilla extract, where the sweet granadilla extract functions as a new neuroprotective agent against autism for the synthesis of *P. ligularis*-AuNPs. The synthesized AuNPs were thoroughly characterized through different techniques including, X-ray diffraction, Zeta potential, EDX, UV-visible absorption, and HRTEM. According to the examination of HRTEM, *P. ligularis*-AuNPs have spherical and triangular forms and have a size range of 8.43–13 nm. The findings demonstrate that *P. ligularis*-AuNPs were more biologically active than pure sweet granadilla extract. The *P. ligularis*-AuNPs had a strong neuroprotective impact on PPA-induced autism in rats. The positive effects were accomplished by reducing neurobehavioral impairment, oxidative stress, and inflammation, improving brain neurotransmitters and neurochemicals, reducing apoptosis, and boosting the antioxidant defense system in the brain. This study may open up possibilities for the environmentally friendly and biologically active green synthesis of gold nanoparticles from *P. ligularis*, which may have a potential therapeutic approach for the treatment of autism. The limitations of the current study have in adequate in the exact mechanism action against autism, which may be challenging to identify additional consequences of chronic use and determine whether the anxiety notice through behavioural analysis, especially connected to brain damage (cerebellar), which also have an influence on emotions and behaviour.

6. Future perspectives

Clinical trials for the treatment of autism are now being investigated worldwide, and recent reports have shown some encouraging progress. Therefore, in context, nanoparticles are considered to be a promising therapeutic agent. Since their exact mechanisms of action are still unknown, AuNPs are a good and powerful antioxidant. The effectiveness of AuNPs has been thoroughly investigated against autism and it has been concluded that their efficiency against autism is sufficient to expand the contribution of this study to include autism nano therapies. However, some investigation on the use of nanoparticles against a few autistic rats has been performed, but the corresponding nanoparticles have not yet been examined to evaluate their impact on autism patients.

Funding

This research did not receive any specific grant from funding agencies in the public, commercial, or not-for-profit sectors.

CRedit authorship contribution statement

Najlaa S. Al-Radadi: Conceptualization, Data curation,

Methodology, Visualization, Software, Investigation, Supervision, Writing – original draft. **Widad M. Al-Bishri**: . **Neveen A. Salem**: Methodology, Software, Writing – original draft. **Shaimaa A. ElShebiny**: .

Declaration of competing interest

The authors declare that they have no known competing financial interests or personal relationships that could have appeared to influence the work reported in this paper.

References:

- Abdelkader, N.F., El-Batal, A.I., Amin, Y.M., Hawas, A.M., Hassan, S.H., Eid, N.I., 2022. Neuroprotective effect of gold nanoparticles and alpha-lipoic acid mixture against radiation-induced brain damage in rats. *Int. J. Mol. Sci.* 23 (17), 9640.
- Abdullah, Al-Radadi N.S., Hussain, T., Faisal, S., Ali Raza Shah, S., 2022. Novel biosynthesis, characterization and bio-catalytic potential of green algae (*Spirogyra hyalina*) mediated silver nanomaterials. *Saudi J Biol Sci.* 29 (1), 411–419. <https://doi.org/10.1016/j.sjbs.2021.09.013>.
- Aji, A., Kunarti, E.S., Santosa, S.J., 2019. Synthesis of gold nanoparticles using p-aminobenzoic acid and p-aminosalicylic acid as reducing agent. *Indonesian Journal of Chemistry.* 19 (1), 68–77. <https://doi.org/10.22146/IJC.26839>.
- Al Jahdaly, B.A., Al-Radadi, N.S., Eldin, G.M.G., Almahri, A., Ahmed, M.K., Shouei, K., et al., 2021. Selenium nanoparticles synthesized using an eco-friendly method: Dye decolorization from aqueous solutions, cell viability, antioxidant, and antibacterial effectiveness. *J. Mater. Res. Technol.* 11, 85–97. <https://doi.org/10.1016/j.jmrt.2020.12.098>.
- Albert-Gascó, H., Ros-Bernal, F., Castillo-Gómez, E., Olucha-Bordonau, F.E., 2020. Map/erk signaling in developing cognitive and emotional function and its effect on pathological and neurodegenerative processes. *Int. J. Mol. Sci.* 21, 1–29. <https://doi.org/10.3390/ijms21124471>.
- Alesaway, N.H., Algobe, S.M., Almarghalani, R.Z., Alasmari, B.G., Alsaedi, A.M., Salem, N. A., 2021. Neurotoxic assessment of chronic abuse of pregabalin in Wistar rats. *Journal of Pharmaceutical Research International.* 33 (27B), 58–66. <https://doi.org/10.9734/jpri/2021/v33i27B31505>.
- Aljabali, A.A.A., Akkam, Y., Al Zoubi, M.S., Al-Batayneh, K.M., Al-Trad, B., Alrob, O.A., et al., 2018. Synthesis of gold nanoparticles using leaf extract of ziziphus zizyphus and their antimicrobial activity. *Nanomaterials* 8 (3). <https://doi.org/10.3390/nano8030174>.
- Al-Radadi, N.S., 2018. Artichoke (*Cynara scolymus* L.) mediated rapid analysis of silver nanoparticles and their utilisation on the cancer cell treatments. *J. Comput. Theor. Nanosci.* 15 (6–7), 1818–1829. <https://doi.org/10.1166/jctn.2018.7317>.
- Al-Radadi, N.S., 2019. Green synthesis of platinum nanoparticles using Saudi's Dates extract and their usage on the cancer cell treatment. *Arab. J. Chem.* 12 (3), 330–349. <https://doi.org/10.1016/j.arabj.2018.05.008>.
- Al-Radadi, N.S., 2021a. Facile one-step green synthesis of gold nanoparticles (AuNp) using licorice root extract: Antimicrobial and anticancer study against HepG2 cell line. *Arab. J. Chem.* 14 (2) <https://doi.org/10.1016/j.arabj.2020.102956>.
- Al-Radadi, N.S., 2021b. Green Biosynthesis of Flaxseed Gold Nanoparticles (Au-NPs) as Potent Anti-cancer Agent Against Breast Cancer Cells. *J. Saudi Chem. Soc.* 25 (6) <https://doi.org/10.1016/j.jscs.2021.101243>.
- Al-Radadi, N.S., 2022a. Microwave assisted green synthesis of Fe@Au core-shell NPs magnetic to enhance olive oil efficiency on eradication of helicobacter pylori (life preserver). *Arab. J. Chem.* 15 (5) <https://doi.org/10.1016/j.arabj.2022.103685>.
- Al-Radadi, N.S., 2022b. Laboratory scale medicinal plants mediated green synthesis of biocompatible nanomaterials and their versatile biomedical applications. *Saudi Journal of Biological Sciences* (29), 3848–3870. <https://doi.org/10.1016/j.sjbs.2022.02.042>.
- Al-Radadi, N.S., 2022c. Saussurea costus for sustainable and eco-friendly synthesis of palladium nanoparticles and their biological activities. *Arab. J. Chem.* 15 (11) <https://doi.org/10.1016/j.arabj.2022.104294>.
- Al-Radadi, N.S., 2022d. Single-step green synthesis of gold conjugated polyphenol nanoparticle using extracts of Saudi's myrrh: Their characterization, molecular docking and essential biological applications. *Saudi Pharmaceutical Journal.* 30 (9), 1215–1242. <https://doi.org/10.1016/j.sjps.2022.06.028>.
- Al-Radadi, N.S., 2022e. Biogenic proficient synthesis of (Au-NPs) via aqueous extract of Red Dragon Pulp and seed oil: Characterization, antioxidant, cytotoxic properties, anti-diabetic anti-inflammatory, anti-Alzheimer and their anti-proliferative potential against cancer cell lines. *Saudi J Biol Sci.* 29 (4), 2836–2855. <https://doi.org/10.1016/j.sjbs.2022.01.001>.
- Al-Radadi, N.S., 2022. Ephedra mediated green synthesis of gold nanoparticles (AuNPs) and evaluation of its antioxidant, antipyretic, anti-asthmatic, and antimicrobial properties. *Arab. J. Chem.* 16 (1) <https://doi.org/10.1016/j.arabj.2022.104353>.
- Al-Radadi, N.S., Abu-Dief, A.M., 2022. Silver nanoparticles (AgNPs) as a metal nanotherapy: possible mechanisms of antiviral action against COVID-19. *Inorganic and Nano-Metal Chemistry.* <https://doi.org/10.1080/24701556.2022.2068585>.
- Al-Radadi, N.S., Adam, S.I.Y., 2020. Green biosynthesis of Pt-nanoparticles from Anbara fruits: Toxic and protective effects on CCl4 induced hepatotoxicity in Wistar rats. *Arab. J. Chem.* 13 (2), 4386–4403. <https://doi.org/10.1016/j.arabj.2019.08.008>.
- Al-Radadi, N.S., Al-Youbi, A.N., 2018a. One-step synthesis of au nano-assemblies and study of their anticancer activities. *J. Comput. Theor. Nanosci.* 15 (6–7), 1861–1870. <https://doi.org/10.1166/jctn.2018.7323>.
- Al-Radadi, N.S., Abdullah, F.S., Alotaibi, A., Ullah, R., Hussain, T., et al., 2022. Zingiber officinale driven bioproduction of ZnO nanoparticles and their anti-inflammatory, anti-diabetic, anti-Alzheimer, anti-oxidant, and anti-microbial applications. *Inorg. Chem. Commun.* <https://doi.org/10.1016/j.inoche.2022.109274>.
- Al-Radadi, N.S., Al-Youbi, A.N., 2018b. Environmentally-safe synthesis of gold and silver nano-particles with AL-madinah Barni fruit and their applications in the cancer cell treatments. *J. Comput. Theor. Nanosci.* 15 (6–7), 1853–1860. <https://doi.org/10.1166/jctn.2018.7322>.
- Amini, F., Amini-Khoei, H., Haratizadeh, S., Setayesh, M., Basiri, M., Raeiszadeh, M., Nozari, M., 2023. Hydroalcoholic extract of *Passiflora incarnata* improves the autistic-like behavior and neuronal damage in a valproic acid-induced rat model of autism. *J. Tradit. Complement. Med.* 1;13(4):315–24 <https://doi.org/10.1016/j.jtcme.2023.02.005>.
- Anadozie, S.O., Effiom, D.O., Adewale, O.B., Jude, J., Zosela, I., Akawa, O.B., Olayinka, J.N., Roux, S., 2023. Hibiscus sabdariffa synthesized gold nanoparticles ameliorate aluminum chloride induced memory deficits through inhibition of COX-2/BACE-1 mRNA expression in rats. *Arab. J. Chem.* 16 (4), 104604 <https://doi.org/10.1016/j.arabj.2023.104604>.
- Annamalai, A., Christina, V.L.P., Sudha, D., Kalpana, M., Lakshmi, P.T.V., 2013. Green synthesis, characterization and antimicrobial activity of Au NPs using *Euphorbia hirta* L. leaf extract. *Colloids Surf. B Biointerfaces* 108, 60–65. <https://doi.org/10.1016/j.colsurfb.2013.02.012>.
- Ashok, A.D., Ravivarman, J., Kayalvizhi, K., 2020. Nutritional Values of Minor Fruits on Immunity Development to Combat Diseases. *Int J Curr Microbiol Appl Sci.* 9 (6), 1303–1311. <https://doi.org/10.20546/ijcm.2020.906.162>.
- Ashwood, P., Krakowiak, P., Hertz-Picciotto, I., Hansen, R., Pessah, I., van de Water, J., 2011. Elevated plasma cytokines in autism spectrum disorders provide evidence of immune dysfunction and are associated with impaired behavioral outcome. *Brain Behav. Immun.* 25 (1), 40–45. <https://doi.org/10.1016/j.bbi.2010.08.003>.
- Avshalumov, M.v., Chen, B.T., Marshall, S.P., Peña, D.M., Rice, M.E., 2003. Glutamate-dependent inhibition of dopamine release in striatum is mediated by a new diffusible messenger. *H202.* 23 (7), 2744–2750. <https://doi.org/10.1523/JNEUROSCI.23-07-02744.2003>.
- Azmitia, E.C., Singh, J.S., Hou, X.P., Wegiel, J., 2011. Dystrophic serotonin axons in postmortem brains from young autism patients. *Anat. Rec.* 294 (10), 1653–1662. <https://doi.org/10.1002/ar.21243>.
- Balasubramanian, S., Kala, S.M.J., Pushparaj, T.L., 2020. Biogenic synthesis of gold nanoparticles using *Jasminum auriculatum* leaf extract and their catalytic, antimicrobial and anticancer activities. *J. Drug Delivery Sci. Technol.* 57 (February), 101620 <https://doi.org/10.1016/j.jddst.2020.101620>.
- Barabadi, H., Webster, T.J., Vahidi, H., Sabori, H., Damavandi Kamali, K., Zajayeri Shoushtari, F., et al., 2020. Green nanotechnology-based gold nanomaterials for hepatic cancer therapeutics: A systematic review. *Iranian Journal of Pharmaceutical Research.* 19, 3–17. <https://doi.org/10.22037/ijpr.2020.113820.14504>.
- Barbosa Santos, T., de Araujo, F.P., Neto, A.F., de Freitas, S.T., de Souza, A.J., de Oliveira Vilar, S.B., et al., 2021. Phytochemical Compounds and Antioxidant Activity of the Pulp of Two Brazilian Passion Fruit Species: *Passiflora Cincinnata* Mast. And *Passiflora Edulis* Sims. *International Journal of Fruit Science.* 21 (1), 255–269. <https://doi.org/10.1080/15538362.2021.1872050>.
- Benincá, J.P., Montanher, A.B., Zucolotto, S.M., Schenkel, E.P., Fröde, T.S., 2007. Evaluation of the anti-inflammatory efficacy of *Passiflora edulis*. *Food Chem.* 104 (3), 1097–1105. <https://doi.org/10.1016/j.foodchem.2007.01.020>.
- Bernard, S., Enayati, A., Roger, H., Binstock, T., Redwood, L., 2002. The role of mercury in the pathogenesis of autism. *Mol. Psychiatry* 7, S42–S43. <https://doi.org/10.1038/sj.mp.4001177>.
- Bhandari, R., Kuhad, A., 2015. Neuropsychopharmacotherapeutic efficacy of curcumin in experimental paradigm of autism spectrum disorders. *Life Sci.* 141, 156–169. <https://doi.org/10.1016/j.lfs.2015.09.012>.
- Bhaskar, S., Tian, F., Stoeger, T., Kreyling, W., de la Fuente, J.M., Grazi, V., et al., 2010. Multifunctional Nanocarriers for diagnostics, drug delivery and targeted treatment across blood-brain barrier: perspectives on tracking and neuroimaging. *Part. Fibre Toxicol.* 7 (1), 1–25. <http://www.particleandfibretoxicology.com/content/7/1/3>.
- Boaventura, B.C.B., di Pietro, P.F., Klein, G.A., Stefanuto, A., de Moraes, E.C., de Andrade, F., et al., 2013. Antioxidant potential of mate tea (*Ilex paraguariensis*) in type 2 diabetic mellitus and pre-diabetic individuals. *J. Funct. Foods* 5 (3), 1057–1064. <https://doi.org/10.1016/j.jff.2013.03.001>.
- Bölte, S., Mahdi, S., de Vries, P.J., Granlund, M., Robison, J.E., Shulman, C., et al., 2019. The Gestalt of functioning in autism spectrum disorder: Results of the international conference to develop final consensus International Classification of Functioning. Disability and Health Core Sets. *Autism.* 23 (2), 449–467. <https://doi.org/10.1177/1362361318755522>.
- Boomi, P., Ganesan, R.M., Poorani, G., Gurumallesu Prabu, H., Ravikumar, S., Jeyakanthan, J., 2019. Biological synergy of greener gold nanoparticles by using *Coleus aromaticus* leaf extract. *Materials Science and Engineering c.* 99, 202–210. <https://doi.org/10.1016/j.msec.2019.01.105>.
- Boruah, J.S., Devi, C., Hazarika, U., Bhaskar Reddy, P.V., Chowdhury, D., Barthakur, M., et al., 2021. Green synthesis of gold nanoparticles using an antiepileptic plant extract: in vitro biological and photo-catalytic activities. *RSC Adv.* 11 (45), 28029–28041. <https://doi.org/10.1039/d1ra02669k>.
- Breerton, C.F., Sutton, C.E., Lalor, S.J., Lavelle, E.C., Mills, K.H.G., 2009. Inhibition of ERK MAPK Suppresses IL-23- and IL-1-Driven IL-17 Production and Attenuates Autoimmune Disease. *J. Immunol.* 183 (3), 1715–1723. <https://doi.org/10.4049/jimmunol.0803851>.

- Bugallo, V.L., Realini, M.F., Facciuto, G.R., Poggio, L., 2020. Karyotypic analyses and genomic affinity among Argentinean species of Passiflora. *Rodriguesia*. 71. <https://doi.org/10.1590/2175-7860202071110>.
- Cañas, N., Gorina, R., Planas, A.M., Vergés, J., Montell, E., García, A.G., et al., 2010. Chondroitin sulfate inhibits lipopolysaccharide-induced inflammation in rat astrocytes by preventing nuclear factor kappa B activation. *Neuroscience* 167 (3), 872–879. <https://doi.org/10.1016/j.neuroscience.2010.02.069>.
- Capasso, A., Sorrentino, L., 2005. Pharmacological studies on the sedative and hypnotic effect of Kava kava and Passiflora extracts combination. *Phytomedicine* 12 (1–2), 39–45. <https://doi.org/10.1016/j.phymed.2004.03.006>.
- Carmona-Hernandez, J.C., Tabora-Ocampo, G., González-Correa, C.H., 2021. Folin-Ciocalteu Reaction Alternatives for Higher Polyphenol Quantitation in Colombian Passion Fruits. *Int. J. Food Sci.* <https://doi.org/10.1155/2021/8871301>.
- Castro, J.R., García-Hernández, L., Ortega, P.A.R., Islas, D.A., 2018. Green synthesis of gold nanoparticles (AuNPs) by *Cupressus goveniana* extract. *ECS Trans.* 84 (1) <https://doi.org/10.1149/08401.0207ecst>.
- Choi, J.H., Kim, K.J., Kim, S., 2016. Comparative Effect of Quercetin and Quercetin-3-O-β-D-Glucoside on Fibrin Polymers, Blood Clots, and in Rodent Models. *J. Biochem. Mol. Toxicol.* 30 (11), 548–558. <https://doi.org/10.1002/jbt.21822>.
- Coleta, M., Campos, M.G., Cotrim, M.D., Proença da Cunha, A., Thieme Verlag Stuttgart, G., York, N., 2001. Comparative evaluation of the elevated plus maze anxiety test. *Pharmacopsychiatry* 34, 20–21. <https://doi.org/10.1055/s-2001-15460>.
- da Fonseca, L.R., Rodrigues, R. de A., Ramos, A. de S., da Cruz, J.D., Ferreira, J.L.P., Silva, J.R. de A., et al., 2020. Herbal medicinal products from passiflora for anxiety: an unexploited potential. *Scientific World Journal* 2020. <https://doi.org/10.1155/2020/6598434>.
- da Silva, B.F., Pérez, S., Gardinalli, P., Singhal, R.K., Mozeto, A.A., Barceló, D., 2011. Analytical chemistry of metallic nanoparticles in natural environments. *TrAC - Trends in Analytical Chemistry*. 30, 528–540. <https://doi.org/10.1016/j.trac.2011.01.008>.
- Das, S., Bag, B.G., Basu, R., 2015. *Abronia augusta* Linn bark extract-mediated green synthesis of gold nanoparticles and its application in catalytic reduction. *Applied Nanoscience (switzerland)*. 5 (7), 867–873. <https://doi.org/10.1007/s13204-014-0384-4>.
- de Oliveira, A.B., de Almeida Lopes, M.M., Moura, C.F.H., de Siqueira, O.L., de Souza, K. O., Filho, E.G., et al., 2017. Effects of organic vs. conventional farming systems on quality and antioxidant metabolism of passion fruit during maturation. *Sci. Hortic.* 222, 84–89. <https://doi.org/10.1016/j.scientia.2017.05.021>.
- Deshmukh, S.P., Patil, S.M., Mullani, S.B., Delekar, S.D., 2019. Silver nanoparticles as an effective disinfectant. *Mater. Sci. Eng. C* 97, 954–965. <https://doi.org/10.1016/j.msec.2018.12.102>.
- Doğan, M., Albayrak, Y., Erbaş, O., 2023. Torasemide improves the propionic acid-induced autism in rats: A histopathological and imaging study. *Alpha Psychiatry*. 24 (1), 22. <https://doi.org/10.5152/alphapsychiatry.2023.22975>.
- Dudhane, A.A., Waghmode, S.R., Dama, L.B., Mhaindarkar, V.P., Sonawane, A., Kataria, S., 2019. Synthesis and characterization of gold nanoparticles using plant extract of *Terminalia arjuna* with antibacterial activity. *International Journal of Nanoscience and Nanotechnology*. 15 (2), 75–82. <http://www.ijnonline.net/&url=http://www.ijnonline.net/article/35418.html>.
- El-Ansary, A., Al-Salem, H.S., Asma, A., Al-Dbass, A., 2017. Glutamate excitotoxicity induced by orally administered propionic acid, a short chain fatty acid can be ameliorated by bee pollen. *Lipids Health Dis.* 16 (1) <https://doi.org/10.1186/s12944-017-0485-7>.
- Ellman, G.L., 1959. Tissue Su-γd-1 Groups. *ARCHIVES OF BIOCHEMISTRY AND BIOPHYSICS*. 82 (1), 70–77. [https://doi.org/10.1016/0003-9861\(59\)90090-6](https://doi.org/10.1016/0003-9861(59)90090-6).
- El-Naggar, M.E., Shaheen, T.I., Fouda, M.M.G., Hebeish, A.A., 2016. Eco-friendly microwave-assisted and rapid synthesis of well-stabilized gold and core-shell silver-gold nanoparticles. *Carbohydr. Polym.* 136, 1128–1136. <https://doi.org/10.1016/j.carbpol.2015.10.003>.
- Faisal, S., Al-Radadi, N.S., Jan, H., Abdullah, S.A.S.A., Shah, S., et al., 2021. Curcuma longa mediated synthesis of copper oxide, nickel oxide and Cu-Ni bimetallic hybrid nanoparticles: Characterization and evaluation for antimicrobial, anti-parasitic and cytotoxic potentials. *Coatings* 11 (7). <https://doi.org/10.3390/coatings11070849>.
- Flores-Méndez, M., Méndez-Flores, O.G., Ortega, A., 2016. Glia plasma membrane transporters: Key players in glutamatergic neurotransmission. *Neurochem. Int.* 98, 46–55. <https://doi.org/10.1016/j.neuint.2016.04.004>.
- Fu, X., Cai, J., Zhang, X., Li, W.D., Ge, H., Hu, Y., 2018. Top-down fabrication of shape-controlled, monodisperse nanoparticles for biomedical applications. *Adv. Drug Deliv. Rev.* 132, 169–187. <https://doi.org/10.1016/j.addr.2018.07.006>.
- Fu, Z., Yang, J., Wei, Y., Li, J., 2016. Effects of piceatannol and pterostilbene against β-amyloid-induced apoptosis on the PI3K/Akt/Bad signaling pathway in PC12 cells. *Food Funct.* 7 (2), 1014–1023. <https://doi.org/10.1039/C5FO01124H>.
- Garnier, C., Roussy, G., Barthelemy, C., Leddet, I., Garreau, B., Muh, J.P., et al., 1986. Dopamine-Beta-Hydroxylase (DBH) and Homovanillic Acid (HVA) in Autistic Children. *J. Autism Dev. Disord.* 16, 23–29. <https://doi.org/10.1007/bf01531575>.
- Gebreslassie, Y.T., Gebretnsae, H.G., 2021. Green and Cost-Effective Synthesis of Tin Oxide Nanoparticles: A Review on the Synthesis Methodologies, Mechanism of Formation, and Their Potential Applications. *Nanoscale Res. Lett.* 16 <https://doi.org/10.1186/s11671-021-03555-6>.
- George, M., Joseph, L., Saji, J., Jilu, S.C., 2017. review on screening of antidiabetic activity of *Passiflora ligularis*. *The Pharma Innovation Journal*. 6 (7), 06–07. <https://www.thepharmajournal.com/archives/2017/vol6issue7/PartA/6-6-33-300.pdf>.
- Geraldes, A.N., da Silva, A.A., Leal, J., Estrada-Villegas, G.M., Lincopan, N., Katti, K.V., et al., 2016. Green Nanotechnology from Plant Extracts: Synthesis and Characterization of Gold Nanoparticles. *Adv Nanopart.* 05 (03), 176–185. <https://doi.org/10.4236/anp.2016.53019>.
- Gnanaprakasam, P., Jeena, S.E., Premnath, D., Selvaraju, T., 2016. Simple and robust green synthesis of Au NPs on reduced graphene oxide for the simultaneous detection of toxic heavy metal ions and bioremediation using bacterium as the scavenger. *Electroanalysis* 28 (8), 1885–1893. <https://doi.org/10.1002/elan.201600002>.
- González-Fraguela, M.E., Hung, M.L.D., Vera, H., Maragoto, C., Noris, E., Blanco, L., et al., 2013. Oxidative stress markers in children with autism spectrum disorders. *Br J Med Res.* 3 (2). <https://files.sld.cu/inmunologia/files/2013/02/gonzalez-fraguela.pdf>.
- Guerrini, G., Ciciani, G., Costanzo, A., Daniele, S., Martini, C., Ghelardini, C., et al., 2013. Synthesis of novel cognition enhancers with pyrazolo[5,1-c][1,2,4] benzotriazine core acting at γ-aminobutyric acid type A (GABAA) receptor. *Bioorg. Med. Chem.* 21 (8), 2186–2198. <https://doi.org/10.1016/j.bmc.2013.02.027>.
- Gurunathan, S., Han, J.W., Park, J.H., Kim, J.H., 2014. A green chemistry approach for synthesizing biocompatible gold nanoparticles. *Nanoscale Res. Lett.* 9 (1), 1–11. <http://www.nanoscalereslett.com/content/9/1/248>.
- Hamelin, M., Varmira, K., Veisi, H., 2018. Green synthesis and characterizations of gold nanoparticles using Thyme and survey cytotoxic effect, antibacterial and antioxidant potential. *J Photochem Photobiol b.* 184, 71–79. <https://doi.org/10.1016/j.jphotobiol.2018.05.016>.
- Han, S., Tai, C., Westenbroek, R.E., Yu, F.H., Cheah, C.S., Potter, G.B., et al., 2012. Autistic-like behaviour in Scn1a +/− mice and rescue by enhanced GABA-mediated neurotransmission. *Nature* 489 (7416), 385–390. <https://doi.org/10.1038/nature11356>.
- Hayretoglu, C., Algedik, P., Ekmekci, C.G., Gunal, O.B., Agyuz, U., Yildirim, H., et al., 2020. Determination of genetic changes in etiology of autism spectrum disorder in twins by whole-exome sequencing. *Gene Rep.* 19. <https://doi.org/10.1016/j.genrep.2020.100618>.
- He, X., Luan, F., Yang, Y., Wang, Z., Zhao, Z., Fang, J., et al., 2020. *Passiflora edulis*: An Insight Into Current Researches on Phytochemistry and Pharmacology. *Frontiers in Pharmacology*. *Frontiers Media* s.a. 11. <https://doi.org/10.3389/fphar.2020.00617>.
- Hogg, S., 1996. A Review of the Validity and Variability of the Elevated Plus-Maze as an Animal Model of Anxiety. *Pharmacol. Biochem. Behav.* 54. [https://doi.org/10.1016/0091-3057\(95\)02126-4](https://doi.org/10.1016/0091-3057(95)02126-4).
- Ijaz, I., Gilani, E., Nazir, A., Bukhari, A., 2020. Detail Review on Chemical, Physical and Green Synthesis, Classification, Characterizations and Applications of Nanoparticles 13, 59–81.
- Ismail, E.H., Saqr, A.M.A., Assirey, E., Naqvi, A., Okasha, R.M., 2018. Successful green synthesis of gold nanoparticles using a corchorus olitorius extract and their antiproliferative effect in cancer cells. *Int. J. Mol. Sci.* 19 (9) <https://doi.org/10.3390/ijms19092612>.
- Jafarizad, A., Safaee, K., Gharibian, S., Omidi, Y., Ekinici, D., 2015. Biosynthesis and In-vitro Study of Gold Nanoparticles Using *Mentha* and *Pelargonium* Extracts. *Procedia Mater. Sci.* 11, 224–230. <https://doi.org/10.1016/j.mspro.2015.11.113>.
- Jawna-Zbońska, K., Blecharz-Klin, K., Joniec-Maciejak, I., Wawer, A., Pyrzanowska, J., Piechal, A., et al., 2016. *Passiflora incarnata* L. Improves Spatial Memory, Reduces Stress, and Affects Neurotransmission in Rats. *Phytother. Res.* 30 (5), 781–789. <https://doi.org/10.1002/ptr.5578>.
- Ji, Y., Cao, Y., Song, Y., 2019. Green synthesis of gold nanoparticles using a *Cordyceps militaris* extract and their antiproliferative effect in liver cancer cells (HepG2). *Artif. Cells Nanomed. Biotechnol.* 47 (1), 2737–2745. <https://doi.org/10.1080/21691401.2019.1629952>.
- Kajani, A.A., Bordbar, A.K., Esfahani, S.H.Z., Razmjou, A., 2016. Gold nanoparticles as potent anticancer agent: green synthesis, characterization, and in vitro study. *RSC Adv.* 6 (68), 63973–63983. <https://doi.org/10.1039/c6ra09050h>.
- Kang, J.P., Kim, Y.J., Singh, P., Huo, Y., Sosnikova, V., Markus, J., et al., 2018. Biosynthesis of gold and silver chloride nanoparticles mediated by *Crataegus pinnatifida* fruit extract: in vitro study of anti-inflammatory activities. *Artif. Cells Nanomed. Biotechnol.* 46 (8), 1530–1540. <https://doi.org/10.1080/21691401.2017.1376674>.
- Karthik, R., Chen, S.M., Elangovan, A., Muthukrishnan, P., Shanmugam, R., Lou, B.S., 2016. Phyto mediated biogenic synthesis of gold nanoparticles using *Cerasus serrulata* and its utility in detecting hydrazine, microbial activity and DFT studies. *J. Colloid Interface Sci.* 468, 163–175. <https://doi.org/10.1016/j.jcis.2016.01.046>.
- Khalil, A., Tazeddinova, D., 2020. The upshot of Polyphenolic compounds on immunity amid COVID-19 pandemic and other emerging communicable diseases: An appraisal. *Natural Products and Bioprospecting*. Springer, 10, 411–429. <https://doi.org/10.1007/s13659-020-00271-z>.
- Khan, S., Bakht, J., Syed, F., 2018. Green synthesis of gold nanoparticles using *Acer pentapomicum* leaves extract its characterization, antibacterial, antifungal and antioxidant bioassay. *Dig. J. Nanomater. Biostruct.* 13 (2), 579–589. https://www.chalcogen.ro/579_KhanS.pdf.
- Khan, T., Ullah, N., Khan, M.A., Mashwani, Z. ur R., Nadhman, A., 2019. Plant-based gold nanoparticles; a comprehensive review of the decade-long research on synthesis, mechanistic aspects and diverse applications. *Adv. Colloid Interface Sci.* 272 <https://doi.org/10.1016/j.cis.2019.102017>.
- Khanbabaee, M., Hughes, E., Ellegood, J., Qiu, L.R., Yip, R., Dobry, J., et al., 2019. Precocious myelination in a mouse model of autism. *Transl. Psychiatry* 9 (1). <https://doi.org/10.1038/s41398-019-0590-7>.
- Khandanlou, R., Murthy, V., Saranath, D., Damani, H., 2018. Synthesis and characterization of gold-conjugated *Backhousia citriodora* nanoparticles and their anticancer activity against MCF-7 breast and HepG2 liver cancer cell lines. *J. Mater. Sci.* 53 (5), 3106–3118. <https://doi.org/10.1007/s10853-017-1756-4>.
- Khandel, P., Yadav, R.K., Soni, D.K., Kanwar, L., Shahi, S.K., 2018. Biogenesis of metal nanoparticles and their pharmacological applications: present status and application

- prospects. *Journal of Nanostructure in Chemistry*. Springer Medizin 8, 217–254. <https://doi.org/10.1007/s40097-018-0267-4>.
- Khera, R., Mehan, S., Bhalla, S., Kumar, S., Alshammari, A., Alharbi, M., Sadhu, S.S., 2022. Guggulsterone mediated JAK/STAT and PPAR-gamma modulation prevents neurobehavioral and neurochemical abnormalities in propionic acid-induced experimental model of autism. *Molecules* 27 (3), 889. <https://doi.org/10.3390/molecules27030889>.
- Kitaura, H., Sands, M.S., Aya, K., Zhou, P., Hirayama, T., Uthgenannt, B., et al., 2004. Marrow Stromal Cells and Osteoclast Precursors Differentially Contribute to TNF- α -Induced Osteoclastogenesis In Vivo. *J. Immunol.* 173 (8), 4838–4846. <https://doi.org/10.4049/jimmunol.173.8.4838>.
- Kujur, A., Daharwal, S.J., 2021. *Bulletin of Environment, Pharmacology and Life Sciences Novel Formulations of Green Synthesized Plant Based Metal Nanoparticles along with their Therapeutic Applications: an Insight to Nano-Green world*. *Env. Pharmacol. Life Sci.* 10 (3), 217–236, 8 doi: 10.1007/s41204-017-0029-4.
- Lasa, M., Abraham, S.M., Boucheron, C., Saklatvala, J., Clark, A.R., 2002. Dexamethasone Causes Sustained Expression of Mitogen-Activated Protein Kinase (MAPK) Phosphatase 1 and Phosphatase-Mediated Inhibition of MAPK p38. *Mol. Cell Biol.* 22 (22), 7802–7811. <https://doi.org/10.1128/MCB.22.22.7802-7811.2002>.
- Latha, D., Prabhu, P., Gnanamoorthy, G., Munusamy, S., Sampurnam, S., Arulvasu, C., et al., 2019. Size-dependent catalytic property of gold nanoparticle mediated by *Justicia adhatoda* leaf extract. *SN Appl Sci.* 1 (1), 1–14. <https://doi.org/10.1007/s42452-018-0148-y>.
- Lee, K.X., Shamel, K., Miyake, M., Kuwano, N., Bt Ahmad Khairudin, N.B., Bt Mohamad, S.E., et al., 2016, 2016. Green synthesis of gold nanoparticles using aqueous extract of *Garcinia mangostana* fruit peels. *J. Nanomater.* 1–7. <https://doi.org/10.1155/2016/8489094>.
- Li, X., Chauhan, A., Sheik, A.M., Patil, S., Chauhan, V., Li, X.M., et al., 2009. Elevated immune response in the brain of autistic patients. *J. Neuroimmunol.* 207 (1–2), 111–116. <https://doi.org/10.1016/j.jneuroim.2008.12.002>.
- Lobzhanidze, G., Japaridze, N., Lordkipanidze, T., Rzaev, F., MacFabe, D., Zhvania, M., 2020. Behavioural and brain ultrastructural changes following the systemic administration of propionic acid in adolescent male rats. *Int. J. Dev. Neurosci.* 80 (2), 139–156. <https://doi.org/10.1002/jdn.10011>.
- MacFabe, D.F., Cain, D.P., Rodriguez-Capote, K., Franklin, A.E., Hoffman, J.E., Boon, F., et al., 2007. Neurobiological effects of intraventricular propionic acid in rats: Possible role of short chain fatty acids on the pathogenesis and characteristics of autism spectrum disorders. *Behav. Brain Res.* 176 (1), 149–169. <https://doi.org/10.1016/j.bbr.2006.07.025>.
- Majumdar, R., Bag, B.G., Ghosh, P., 2016. *Mimusops elengi* bark extract mediated green synthesis of gold nanoparticles and study of its catalytic activity. *Applied Nanoscience (switzerland)*. 6 (4), 521–528. <https://doi.org/10.1007/s13204-015-0454-2>.
- Mandic-Maravic, V., Grujicic, R., Milutinovic, L., Munjiza-Jovanovic, A., Pejovic-Milovancevic, M., 2022. Dopamine in autism spectrum disorders—focus on D2/D3 partial agonists and their possible use in treatment. *Front. Psych.* 12, 787097. <https://doi.org/10.3389/fpsy.2021.787097>.
- Marklund, S.L., Adolfsson, R., Gottfries, C.G., Winblad, B., 1985. Superoxide Dismutase Isoenzymes in Normal Brains and in Brains from Patients with Dementia of Alzheimer Type. *J. Neurol. Sci.* 67 (3), 319–325. [https://doi.org/10.1016/0022-510X\(85\)90156-X](https://doi.org/10.1016/0022-510X(85)90156-X).
- Meguid, N.A., Dardir, A.A., Abdel-Raouf, E.R., Hashish, A., 2011. Evaluation of oxidative stress in autism: Defective antioxidant enzymes and increased lipid peroxidation. *Biol. Trace Elem. Res.* 143 (1), 58–65. <https://doi.org/10.1007/s12011-010-8840-9>.
- Mehan, S., Rahi, S., Tiwari, A., Kapoor, T., Rajdev, K., Sharma, R., Khera, H., Kosey, S., Kukkar, U., Dudi, R., 2020. Adenylate cyclase activator forskolin alleviates intracerebroventricular propionic acid-induced mitochondrial dysfunction of autistic rats. *Neural Regen. Res.* 15(6):1140.
- Michel, K., Zhao, T., Karl, M., Lewis, K., Fyffe-Maricich, S.L., 2015. Translational control of myelin basic protein expression by ERK2 MAP kinase regulates timely remyelination in the adult brain. *J. Neurosci.* 35 (20), 7850–7865. <https://doi.org/10.1523/JNEUROSCI.4380-14.2015>.
- Milaneze, B., Keijok, W., Jairo, O., Brunelli, P., Janine, B., Larissa, L., Adilson, P., Denise, E., Maria, P., Moises, R., Breno, N., Marco, G., 2014. The green synthesis of gold nanoparticle using extract of *Virola oleifera*. *BMC Proc.* 8 (4). <http://www.biomedcentral.com/1753-6561/8/S4/P29>.
- Miri, A., Darroudi, M., Entezari, R., Sarani, M., 2018. Biosynthesis of gold nanoparticles using *Prosopis farcta* extract and its in vitro toxicity on colon cancer cells. *Res. Chem. Intermed.* 44 (5), 3169–3177. <https://doi.org/10.1007/s11164-018-3299-y>.
- Mirza, R., Sharma, B., 2019. A selective peroxisome proliferator-activated receptor- γ agonist benefited propionic acid induced autism-like behavioral phenotypes in rats by attenuation of neuroinflammation and oxidative stress. *Chem. Biol. Interact.* 311. <https://doi.org/10.1016/j.cbi.2019.108758>.
- Mohamed, M.S., Veeranarayanan, S., Poulouse, A.C., Nagaoka, Y., Minegishi, H., Yoshida, Y., et al., 2014. Type 1 ribotoxin-curcumin conjugated biogenic gold nanoparticles for a multimodal therapeutic approach towards brain cancer. *Biochimica Et Biophysica Acta (BBA)*. 1840 (6), 1657–1669. <https://doi.org/10.1016/j.bbagen.2013.12.020>.
- Moldovan, R., Mitrea, D.R., Florea, A., Chiş, I.C., Suci, Ş., David, L., Moldovan, B.E., Mureşan, L.E., Lenghel, M., Ungur, R.A., Oprea, R.V., 2022. Effects of Gold Nanoparticles Functionalized with Bioactive Compounds from *Cornus mas* Fruit on Aorta Ultrastructural and Biochemical Changes in Rats on a Hyperlipid Diet—A Preliminary Study. *Antioxidants*. 11 (7), 1343. <https://doi.org/10.3390/antiox11071343>.
- Moore, J.A., Chow, J.C.L., 2021. Recent progress and applications of gold nanotechnology in medical biophysics using artificial intelligence and mathematical modeling. *Nano Express*. 2 (2) <https://doi.org/10.1088/2632-959X/abddd3>.
- Moretti, P., Bouwknegt, J.A., Teague, R., Paylor, R., Zoghbi, H.Y., 2005. Abnormalities of social interactions and home-cage behavior in a mouse model of Rett syndrome. *Hum. Mol. Genet.* 14 (2), 205–220. <https://doi.org/10.1093/hmg/ddi016>.
- Mori, T., Wang, X., Aoki, T., Lo, E.H., 2002. Downregulation of Matrix Metalloproteinase-9 and Attenuation of Edema via Inhibition of ERK Mitogen Activated Protein Kinase in Traumatic Brain Injury. *J. Neurotrauma* 19 (11). <https://doi.org/10.1089/089771502320914642>.
- Murad, U., Khan, S.A., Ibrar, M., Ullah, S., Khattak, U., 2018. Synthesis of silver and gold nanoparticles from leaf of *Litchi chinensis* and its biological activities. *Asian Pac. J. Trop. Biomed.* 8 (3), 142. <https://doi.org/10.4103/2221-1691.227995>.
- Oblak, A.L., Gibbs, T.T., Blatt, G.J., 2011. Reduced GABAA receptors and benzodiazepine binding sites in the posterior cingulate cortex and fusiform gyrus in autism. *Brain Res.* 1380, 218–228. <https://doi.org/10.1016/j.brainres.2010.09.021>.
- Olawale, F., Oladimeji, O., Ariatti, M., Singh, M., 2022. Emerging Roles of Green-Synthesized Chalcogen and Chalcoenide Nanoparticles in Cancer Theranostics. *J. Nanotechnol.* 2022. <https://doi.org/10.1155/2022/6176610>.
- Olczak, M., Duszczek, M., Mierzejewski, P., Wierzb-Bobrowicz, T., Dorota Majewska, M., Curie, M., et al., 2010. Lasting neuropathological changes in rat brain after intermittent neonatal administration of thimerosal. *Folia Neuropathol.* 48 (4), 258–269. <https://www.termedia.pl/Original-paper-Lasting-neuropathological-changes-in-rat-brain-after-intermittent-neonatal-administration-of-thimerosal,20,15811,0,1.html>.
- Panzarini, E., Mariano, S., Carata, E., Mura, F., Rossi, M., Dini, L., 2018. Intracellular transport of silver and gold nanoparticles and biological responses: An update. *Int. J. Mol. Sci.* 19. <https://doi.org/10.3390/ijms19051305>.
- Patra, J.K., Baek, K.H., 2015. Novel green synthesis of gold nanoparticles using *Citrus aurantium* rind and investigation of proteasome inhibitory activity, antibacterial, and antioxidant potential. *Int. J. Nanomed.* 10, 7253–7264. <https://doi.org/10.2147/IJN.S95483>.
- Paul, K., Bag, B.G., Samanta, K., 2014. Green coconut (*Cocos nucifera* Linn) shell extract mediated size controlled green synthesis of polyshaped gold nanoparticles and its application in catalysis. *Applied Nanoscience (switzerland)*. 4 (6), 769–775. <https://doi.org/10.1007/s13204-013-0261-6>.
- Pham, T.A., Choi, B.C., Lim, K.T., Jeong, Y.T., 2011. A simple approach for immobilization of gold nanoparticles on graphene oxide sheets by covalent bonding. *Appl. Surf. Sci.* 257 (8), 3350–3357. <https://doi.org/10.1016/j.apsusc.2010.11.023>.
- Placer, Z.A., Cushman, L.L., Connor, B., 1966. Estimation of Product of Lipid Peroxidation (Malonyl Dialdehyde). *Biochemical Systems*. 16 (2), 359–364. [https://doi.org/10.1016/0003-2697\(66\)90167-9](https://doi.org/10.1016/0003-2697(66)90167-9).
- Prakash Patil, M., Kim, J.O., Seo, Y.B., Kang, M.J., Kim, G.D., 2021. Biogenic Synthesis of Metallic Nanoparticles and Their Antibacterial Applications. *Journal of Life Science*. 31 (9), 862–872. <https://doi.org/10.5352/JLS.2021.31.9.862>.
- Quednow, B.B., Kühn, K.U., Hoenig, K., Maier, W., Wagner, M., 2004. Prepulse inhibition and habituation of acoustic startle response in male MDMA ('Ecstasy') users, cannabis users, and healthy controls. *Neuropsychopharmacology* 29 (5), 982–990. <https://doi.org/10.1038/sj.npp.1300396>.
- Quesada, A., Lee, B.Y., Micevych, P.E., 2008. PI3 kinase/Akt activation mediates estrogen and IGF-1 niral DA neuronal neuroprotection against a unilateral rat model of Parkinson's disease. *Dev. Neurobiol.* 68 (5), 632–644. <https://doi.org/10.1002/dne.20609>.
- Rai, S., Nagar, J.C., Mukim, M., 2022. Pharmacological and Medicinal Importance of *Passiflora Edulis*. *International Journal of Research*. 9 (4), 341–349.
- Rajeshkumar, S., Sherif, M.H., Malarkodi, C., Ponnaniakamideen, M., Arasu, M.V., Al-Dhabi, N.A., et al., 2021. Cytotoxicity behaviour of response surface model optimized gold nanoparticles by utilizing fucoidan extracted from *padina tetrastrum*. *J. Mol. Struct.* 1228. <https://doi.org/10.1016/j.molstruc.2020.129440>.
- Ramakrishna, M., Rajesh Babu, D., Gengan, R.M., Chandra, S., Nageswara, R.G., 2016. Green synthesis of gold nanoparticles using marine algae and evaluation of their catalytic activity. *J. Nanostructure Chem.* 6 (1), 1–13. <https://doi.org/10.1007/s40097-015-0173-y>.
- Ramli, A.N.M., Manap, N.W.A., Bhuyar, P., Azelee, N.I.W., 2020. Passion fruit (*Passiflora edulis*) peel powder extract and its application towards antibacterial and antioxidant activity on the preserved meat products. *SN Appl Sci.* 2 (10) <https://doi.org/10.1007/s42452-020-03550-z>.
- Ratan, Z.A., Haidere, M.F., Nurunnabi, M., Shahriar, S.M., Ahammad, A.J.S., Shim, Y.Y., et al., 2020. Green chemistry synthesis of silver nanoparticles and their potential anticancer effects. *Cancers* 12. <https://doi.org/10.3390/cancers12040855>.
- Ravi, M., 2021. The active compounds of *Passiflora spp* and their potential medicinal uses from both in vitro and in vivo evidences. *J. Adv. Biomed. & Pharm. Sci. J. Adv. Biomed. & Pharm. Sci.* 4 (1) <https://doi.org/10.21608/jabps.2020.44321.1105>.
- Rónavári, A., Igaz, N., Adamecz, D.I., Szerencsés, B., Molnar, C., Kónya, Z., et al., 2021. Green silver and gold nanoparticles: Biological synthesis approaches and potentials for biomedical applications. *Molecules* 26 (4). <https://doi.org/10.3390/molecules26040844>.
- Rozhin, A., Batasheva, S., Kruchkova, M., Cherednichenko, Y., Rozhina, E., Fakhru'llin, R., 2021. Biogenic silver nanoparticles: Synthesis and application as antibacterial and antifungal agents. *Micromachines* 12. <https://doi.org/10.3390/mi12121480>.
- Ryals, J.B., Knight, P.R., Stafne, E.T., 2020. Rooting response of seven passion fruit species to basal application of Auxin. *HortTechnology* 30 (6), 692–696. <https://doi.org/10.21273/HORTTECH04660-20>.

- Sachan, A.K., Gupta, A., 2015. A review on nanotized herbal drugs. *Int. J. Pharm. Sci. Res.* 6 (3) <https://doi.org/10.13040/IJPSR.0975>.
- Salem, N.A., Assaf, N., Ismail, M.F., Khadrawy, Y.A., Samy, M., 2016. Ozone Therapy in Ethidium Bromide-Induced Demyelination in Rats: Possible Protective Effect. *Cell. Mol. Neurobiol.* 36 (6), 943–954. <https://doi.org/10.1007/s10571-015-0279-2>.
- Salem, N.A., El-Shamarka, M., Khadrawy, Y., El-Shebiny, S., 2018. New prospects of mesenchymal stem cells for ameliorating temporal lobe epilepsy. *Inflammopharmacology* 26 (963–72). <https://doi.org/10.1007/s10787-018-0456-2>.
- Sampaio, R.F., da Cruz, L.V., Bungart, G.A.M., Correia, L.D.B., Tobal, T.M., 2022. Flour of Winged-stem Passion Fruit Peel: Nutritional Composition, Incorporation in Cookies, and Sensory Acceptability. *Braz. Arch. Biol. Technol.* 65 <https://doi.org/10.1590/1678-4324-2022200776>.
- Saravanan, S., Parimelazhagan, T., 2014. In vitro antioxidant, antimicrobial and anti-diabetic properties of polyphenols of *Passiflora ligularis* Juss. fruit pulp. *Food Sci. Human Wellness* 3 (2), 56–64. <https://doi.org/10.1016/j.fshw.2014.05.001>.
- Sato, A., Tagai, N., Ogino, Y., Uozumi, H., Kawakami, S., Yamamoto, T., Tanuma, S.I., Maruki-Uchida, H., Mori, S., Morita, M., 2022. Passion fruit seed extract protects beta-amyloid-induced neuronal cell death in a differentiated human neuroblastoma SH-SY5Y cell model. *Food Sci. Nutr.* 10 (5), 1461–1468. <https://doi.org/10.1002/fsn3.2757>.
- Satzer, P., Svec, F., Sekot, G., Jungbauer, A., 2016. Protein adsorption onto nanoparticles induces conformational changes: Particle size dependency, kinetics, and mechanisms. *Eng. Life Sci.* 16 (3), 238–246. <https://doi.org/10.1002/elsc.201500059>.
- Sayago-Ayerdi, S., García-Martínez, D.L., Ramírez-Castillo, A.C., Ramírez-Concepción, H. R., Viuda-Martos, M., 2021. Tropical fruits and their co-products as bioactive compounds and their health effects. *Foods* 10 (8) <https://doi.org/10.3390/foods10081952>.
- Schröfel, A., Kratošová, G., Šafařík, I., Šafaříková, M., Raška, I., Šhor, L.M., 2014. Applications of biosynthesized metallic nanoparticles. *Acta Biomaterialia*. Elsevier Ltd. 10, 4023–4042. <https://doi.org/10.1016/j.actbio.2014.05.022>.
- Sharma, P.K., Agrawal, M., Kumar, M.A., Rajagopala, S., 2019. Management Of Autism Spectrum Disorder With Abhayaghrta And Pancha Bhautika Tailanasya-A Case Report. *International Journal of Ayurveda and Pharma Research* 7 (5), 17–22. <http://ijaprs.com/index.php/ijapr/article/view/1176>.
- Shedbalkar, U., Singh, R., Wadhvani, S., Gaidhani, S., Chopade, B.A., 2014. Microbial synthesis of gold nanoparticles: Current status and future prospects. *Adv. Colloid Interface Sci.* 209, 40–48. <https://doi.org/10.1016/j.cis.2013.12.011>.
- Shinde, A., Ganu, J., Naik, P., 2012. Effect of Free Radicals & Antioxidants on Oxidative Stress. *Journal of Dental & Allied Sciences* 1 <https://doi.org/10.4103/2277-4696.159144>.
- Shultz, S.R., MacFabe, D.F., Foley, K.A., Taylor, R., Cain, D.P., 2011. A single mild fluid percussion injury induces short-term behavioral and neuropathological changes in the Long-Evans rat: Support for an animal model of concussion. *Behav. Brain Res.* 224 (2), 326–335. <https://doi.org/10.1016/j.bbr.2011.06.012>.
- Sibuyi, N.R.S., Moabelo, K.L., Fadaka, A.O., Meyer, S., Onani, M.O., Madiehe, A.M., et al., 2021. Multifunctional Gold Nanoparticles for Improved Diagnostic and Therapeutic Applications: A Review. *Nanoscale Res. Lett.* 16 <https://doi.org/10.1186/s11671-021-03632-w>.
- Silverman, J.L., Yang, M., Lord, C., Crawley, J.N., 2010. Behavioural phenotyping assays for mouse models of autism. *Nat. Rev. Neurosci.* 11, 490–502. <https://doi.org/10.1038/nrn2851>.
- Singh, P., Ahn, S., Kang, J.P., Veronika, S., Huo, Y., Singh, H., et al., 2018b. In vitro anti-inflammatory activity of spherical silver nanoparticles and monodisperse hexagonal gold nanoparticles by fruit extract of *Prunus serrulata*: a green synthetic approach. *Artif. Cells Nanomed. Biotechnol.* 46 (8), 2022–2032. <https://doi.org/10.1080/21691401.2017.1408117>.
- Singh, H., Du, J., Singh, P., Yi, T.H., 2018a. Ecofriendly synthesis of silver and gold nanoparticles by *Euphrasia officinalis* leaf extract and its biomedical applications. *Artif. Cells Nanomed. Biotechnol.* 46 (6), 1163–1170. <https://doi.org/10.1080/21691401.2017.1362417>.
- Sun, J., Nan, G., 2017. The extracellular signal-regulated kinase 1/2 pathway in neurological diseases: A potential therapeutic target. *Int. J. Mol. Med.* 39 (6), 1338–1346. <https://doi.org/10.3892/ijmm.2017.2962>.
- Sun, W., Shahrajabian, M.H., Cheng, Q., 2021. Natural dietary and medicinal plants with anti-obesity therapeutics activities for treatment and prevention of obesity during lockdown and in post-COVID-19 era. *Appl. Sci.* 11 (17), 7889. <https://doi.org/10.3390/app11177889>.
- Sunayana, N., Uzma, M., Dhanwini, R.P., Govindappa, M., Prakash, H.S., Vinay, R.B., 2020. Green synthesis of gold nanoparticles from *Vitex negundo* leaf extract to inhibit lipopolysaccharide-induced inflammation through in vitro and in vivo. *J. Clust. Sci.* 31 (2), 463–477. <https://doi.org/10.1007/s10876-019-01661-1>.
- Tannock, I.F., Hot, D., 1989. Acid pH in Tumors and Its Potential for Therapeutic Exploitation. *Cancer Res.* 49 (16), 4373–4384. <http://aacrjournals.org/cancerres/article-pdf/49/16/4373/2435947/cr0490164373.pdf>.
- Tiwari, A., Khera, R., Rahi, S., Mehan, S., Makeen, H.A., Khormi, Y.H., Rehman, M.U., Khan, A., 2021. Neuroprotective effect of α -mangostin in ameliorating propionic acid-induced experimental model of autism in Wistar rats. *Brain Sci.* 11 (3), 288. <https://doi.org/10.3390/brainsci11030288>.
- Vargas, D.L., Nascimbene, C., Krishnan, C., Zimmerman, A.W., Pardo, C.A., 2005. Neuroglial activation and neuroinflammation in the brain of patients with autism. *Ann. Neurol.* 57 (1), 67–81. <https://doi.org/10.1002/ana.20315>.
- Vo, T.T., Nguyen, T.T.N., Huynh, T.T.T., Vo, T.T.T., Nguyen, T.T.N., Nguyen, D.T., et al., 2019. Biosynthesis of silver and gold nanoparticles using aqueous extract from crinum latifolium leaf and their applications forward antibacterial effect and wastewater treatment. *J. Nanomater.* 2019 <https://doi.org/10.1155/2019/8385935>.
- Wahab, A.W., Karim, A., Asmawati, S.I.W., 2018. Bio-synthesis of gold nanoparticles through bioreduction using the aqueous extract of *Muntingia calabura* L. leaves. *Orient. J. Chem.* 34 (1), 401–409. <https://doi.org/10.13005/ojc/340143>.
- Waldmeier, P.C., Kaupmann, K., Urwyler, S., 2008. Roles of GABA_B receptor subtypes in presynaptic auto- and heteroreceptor function regulating GABA and glutamate release. *J. Neural Transm.* 115 (10), 1401–1411. <https://doi.org/10.1007/s00702-008-0095-7>.
- Wen, H., Fu, Z., Wei, Y., Zhang, X., Ma, L., Gu, L., et al., 2018. Antioxidant activity and neuroprotective activity of stilbenoids in rat primary cortex neurons via the PI3K/Akt signalling pathway. *Molecules* 23 (9). <https://doi.org/10.3390/molecules23092328>.
- Yaqoob, S.B., Adnan, R., Rameez Khan, R.M., Gold, R.M., 2020. Silver, and Palladium Nanoparticles: A Chemical Tool for Biomedical Applications. *Frontiers in Chemistry*. Frontiers Media s.a. 8 <https://doi.org/10.3389/fchem.2020.00376>.
- Yucel, N., Bulus, E., Bulus, G.S., Khan, A., Xhibo, F., Turan, S., et al., 2020. Synthesis and Characterization of Novel Nanomaterials for SERS Biomedical. *Journal of Materials and Electronic Devices*. 4.
- Yufune, S., Satoh, Y., Takamatsu, I., Ohta, H., Kobayashi, Y., Takaenoki, Y., et al., 2015. Transient blockade of ERK phosphorylation in the critical period causes autistic phenotypes as an adult in mice. *Sci. Rep.* 5 <https://doi.org/10.1038/srep10252>.
- Zeraik, M.L., Serteyn, D., Deby-Dupont, G., Wauters, J.N., Tits, M., Yariwake, J.H., et al., 2011. Evaluation of the antioxidant activity of passion fruit (*Passiflora edulis* and *Passiflora alata*) extracts on stimulated neutrophils and myeloperoxidase activity assays. *Food Chem.* 128 (2), 259–265. <https://doi.org/10.1016/j.foodchem.2011.03.001>.
- Zhou, Y., Danbolt, N.C., 2014. Glutamate as a neurotransmitter in the healthy brain. *J. Neural Transm.* 121 (8), 799–817. <https://doi.org/10.1007/s00702-014-1180-8>.
- Zibadi, S., Watson, R.R., 2004. Passion Fruit (*Passiflora edulis*) Composition, Efficacy and Safety. *Evid Based Integrative Med.* 1 (3), 183–187. <https://doi.org/10.2165/01197065-200401030-00005>.
- Zimmerman, A.W., Jyonouchi, H., Comi, A.M., Connors, S.L., Milstien, S., Varsou, A., et al., 2005. Cerebrospinal fluid and serum markers of inflammation in autism. *Pediatr. Neurol.* 33 (3), 195–201. <https://doi.org/10.1016/j.pediatrneurol.2005.03.014>.
- Zoroglu, S.S., Armutcu, F., Ozen, S., Gurel, A., Sivasli, E., Yetkin, O., et al., 2004. Increased oxidative stress and altered activities of erythrocyte free radical scavenging enzymes in autism. *Eur. Arch. Psychiatry Clin. Neurosci.* 254 (3), 143–147. <https://doi.org/10.1007/s00406-004-0456-7>.